



SPE 90390

## Modeling Conformance as Dispersion

Coats, K.H., Coats Engineering, Whitson, C.H., NTNU & PERA, Thomas, L.K., ConocoPhillips

Copyright 2004, Society of Petroleum Engineers Inc.

This paper was prepared for presentation at the SPE Annual Technical Conference and Exhibition held in Houston, Texas, U.S.A., 26–29 September 2004.

This paper was selected for presentation by an SPE Program Committee following review of information contained in a proposal submitted by the author(s). Contents of the paper, as presented, have not been reviewed by the Society of Petroleum Engineers and are subject to correction by the author(s). The material, as presented, does not necessarily reflect any position of the Society of Petroleum Engineers, its officers, or members. Papers presented at SPE meetings are subject to publication review by Editorial Committees of the Society of Petroleum Engineers. Electronic reproduction, distribution, or storage of any part of this paper for commercial purposes without the written consent of the Society of Petroleum Engineers is prohibited. Permission to reproduce in print is restricted to a proposal of not more than 300 words; illustrations may not be copied. The proposal must contain conspicuous acknowledgment of where and by whom the paper was presented. Write Librarian, SPE, P.O. Box 833836, Richardson, TX 75083-3836, U.S.A., fax 01-972-952-9435.

### Summary

For decades the effect of physical dispersion (in-situ mixing) in porous media has been of interest in reservoir engineering and groundwater hydrology. Dispersion can affect the development of multi-contact miscibility and bank breakdown in enriched gas drives and miscible solvent floods of any mobility ratio.

The magnitude or extent of dispersion is quantified by the rock property physical dispersivity ( $\alpha$ ) which is the order of 0.01 ft for consolidated rocks and several times smaller for sand-packs, from many laboratory measurements.

Numerical studies of the effect of dispersion on enriched gas drives and field tracer tests often use input values of dispersivity 100 to 1000 or more times larger than  $\sim 0.01$  ft. These large input dispersivity values stem from large apparent dispersivities ( $\alpha_a$ ) determined by matching the one-dimensional convection-diffusion (1D CD) equation to production well effluent tracer concentration profiles observed in field tracer tests.

The large apparent dispersivities reflect conformance or other behavior not governed by the 1D CD equation and should not be used to justify large physical dispersivity as input to numerical studies. This paper shows that large apparent dispersivities observed in field tests can result with physical dispersivity no larger  $\sim 0.01$  ft lab-measured value.

Heterogeneity alone (no physical dispersivity or molecular diffusion) causes no in-situ mixing and cannot explain observed large apparent echo dispersivities. Large apparent echo dispersivities for two reported field tracer tests are shown to result from the effect of drift alone with no dispersion.

The widely reported scale-dependence of apparent dispersivity is a simple and necessary consequence of misapplying the 1D CD equation, with its single parameter of Peclet number  $L/\alpha$ , to conformance it does not describe. Apparent dispersivity is scale-dependent but physical dispersivity is a rock property independent of scale and time.

### Introduction

This paper differentiates between the rock property *physical dispersivity* ( $\alpha$ ), associated with *dispersion* (in-situ mixing), and *apparent dispersivity* ( $\alpha_a$ ) associated with *conformance*. Apparent dispersivities  $\alpha_a$  are determined by a best-fit match of the 1D CD equation to effluent concentration profiles  $C$  vs pore volumes injected  $Q_D$  from field tracer tests or numerical simulations. For the assumptions used in this paper, conformance reflects the combined effects of heterogeneity, well areal pattern and completion intervals, and drift (regional flow gradient).

The  $\alpha_a$  values derived from field tracer test data appear to be strongly scale-dependent<sup>1,2</sup>, with log-log plots of  $\alpha_a$  vs scale  $L$  showing a slope of roughly 1. Field-scale  $\alpha_a$  values are orders of magnitude larger than lab-measured dispersivities<sup>3</sup>  $\alpha \sim 0.01$  ft which have no scale dependence.

Our concern, and the reason for this paper, is the use of large apparent dispersivity values as input physical dispersivity in numerical studies<sup>2,4-8</sup> designed to quantify the impact of dispersion on reservoir processes<sup>a</sup>. The above-referenced studies use input dispersivity values as large as 8000 times larger than a physical dispersivity  $\sim 0.01$  ft. Nearly 40 years ago, Mercado<sup>9</sup> showed that large apparent dispersivities from transmission (two-well) field tracer tests reflected conformance (heterogeneity), not dispersion. We argue that dispersivity  $\sim 0.01$  ft should be input in studies designed to quantify the impact of physical dispersion on reservoir processes.

We show in this paper that apparent dispersivities are approximately the sum of physical dispersivity ( $\alpha$ ) and apparent dispersivity due only to *conformance* ( $\alpha_{ac}$ ),  $\alpha_a \approx \alpha + \alpha_{ac}$ . For all cases of practical interest,  $\alpha_{ac} \gg \alpha$ , making  $\alpha_a \approx \alpha_{ac}$  an excellent approximation. We also show that  $\alpha_{ac} \approx \alpha_{ap} + \alpha_{as}$ , where  $\alpha_{ap}$  is the apparent dispersivity due to pattern (areal) sweep alone, and  $\alpha_{as}$  is the apparent dispersivity due to stratification (vertical) sweep alone.

The literature gives considerable attention to the scale dependence of apparent dispersivities. We show that this is a necessary and expected consequence of matching the 1D CD equation<sup>b</sup>, which describes dispersion, to effluent concentration profiles, which reflect conformance. With very

<sup>a</sup> These reservoir processes include solvent floods and enriched gas drives of any mobility ratio, tracer tests, bank or slug breakdown, and chemical reactions.

<sup>b</sup> The single parameter in this equation is the Peclet number  $N_{Pe} = L/\alpha$ .

few exceptions, there is no physical meaning or significance to this scale-dependence.

Some authors state or imply that heterogeneity causes in-situ mixing<sup>2,6,10</sup>. We argue that heterogeneity alone ( $\alpha=\alpha_t=D_0=0$ ) causes *no* in-situ mixing – a fact we believe has been a long-recognized tenet of reservoir engineering.

Several studies<sup>1,10,11</sup> use zero input dispersivities when numerically simulating heterogeneous systems for the purpose of generating apparent dispersivities. These results reflect *only* conformance and any numerical dispersion present. The magnitude of the generated apparent dispersivities, their scale-dependence and relation to heterogeneities have nothing to do with dispersion or physical dispersivity – heterogeneity alone causes no in-situ mixing.

Numerical simulation results were recently reported<sup>2</sup> for echo and transmission tests that can be interpreted with large, scale-dependent, apparent dispersivity  $\alpha_a$ , and large “local” dispersivities determined from gridblock  $C(t)$  profiles. We show that these results are influenced by numerical dispersion. We also show that these results illustrate the additive-dispersivity approximation.

Large apparent dispersivities observed in field echo (single-well) tests<sup>12</sup>, up to 3 ft, have yet to be explained in the literature using a physical model. We show that large  $\alpha_a$  values in echo tests can result from natural drift and/or transverse dispersion in laminations with contrasting permeabilities.

**Assumptions, Definitions, and Methods**

Except where otherwise noted, assumptions in this paper are as follows. We consider unit-mobility ratio displacements in a porous medium of any heterogeneity, dimensionality, and geometry. Injected (displacing) and original (displaced) fluids have equal viscosities and densities, are incompressible, and obey the law of additive volumes. Wells are vertical and fully penetrating. Darcy flow and uniform porosity and formation thickness are assumed. These displacements include, on lab or field scale, tracer tests and first-contact miscible (solvent) floods. Effects of tracer adsorption and degradation are neglected.

We begin with some key definitions. We also describe methods for modeling laboratory and field tests designed to measure physical dispersivity and/or conformance.

**Concentration and Effluent Profile.** For field tracer tests, *concentration*  $C$  is tracer concentration, normalized by initial injected tracer concentration. For miscible solvent floods,  $C$  is fraction of solvent in solvent-oil mixtures. *Affluent profile* or *profile* is the production wellstream  $C$  vs time or pore volumes injected resulting from an injection process.

A clear distinction should be made between in-situ and *effluent* concentrations. Mixing in the reservoir is associated with in-situ concentrations. Mixing in the wellbore and surface facilities is associated with wellstream effluent concentration (a weighted average of flowing concentrations<sup>7</sup>).

**Physical Dispersion.** The terms *physical dispersion* and *dispersion* are used interchangeably to denote the in-situ mixing attributable to dispersion coefficients<sup>3</sup>  $K_l$  and  $K_t$  (Eq. 5) in the presence of flow and/or concentration gradients. In

modeling, in-situ mixing should not occur if these coefficients are input as zero.

**Physical Dispersivity.** Physical dispersivity  $\alpha$  is a rock property determined from flow tests using laboratory coreplugs or sand-packs which are homogeneous or nearly so. The terms *physical dispersivity* and *dispersivity* are used interchangeably. Two dispersivities exist (relative to flow direction): *longitudinal*  $\alpha$  and *transverse*  $\alpha_t$ . Dispersivity is a microstructural<sup>9</sup> rock property related to irregularities in pore structure at the level of pore dimensions. Physical dispersivity is neither time-dependent nor scale-dependent, regardless of whether scale is defined as system length, distance traveled, or “scale of heterogeneity”.

Perkins and Johnston<sup>3</sup> give an “average” longitudinal  $\alpha=0.006$  ft (0.18 cm) for sandstones, and transverse  $\alpha_t$  30 times less; they give significantly smaller  $\alpha$  values for unconsolidated sand. Others report lab-measured dispersivities ~0.01 ft and transverse dispersivities some 10-100 times less.

**Convection-Dispersion (CD) Equations.** For a one-dimensional miscible displacement in a homogeneous porous medium, the concentration profile in time and distance is<sup>13</sup>

$$C = \frac{1}{2} \operatorname{erfc} \left( \frac{x_D - Q_D}{2\sqrt{Q_D/N_{Pe}}} \right) + \frac{e^{x_D N_{Pe}}}{2} \operatorname{erfc} \left( \frac{x_D + Q_D}{2\sqrt{Q_D/N_{Pe}}} \right) \dots\dots\dots (1)$$

*erfc* is the complimentary error function,  $\operatorname{erfc}(a)=1-\operatorname{erf}(a)$ ,  $x_D$  is the dimensionless distance traveled,  $x/L$ ,  $Q_D$  is the dimensionless pore volumes injected and  $N_{Pe}$  is the dimensionless Peclet number given by  $N_{Pe}=uL/K_l$ . Defining longitudinal dispersivity  $\alpha=K_l/u$ , where  $K_l$  is the longitudinal dispersion coefficient, gives

$$\alpha = \frac{1}{N_{Pe}} L \dots\dots\dots (2)$$

Considering the effluent concentration profile at  $x=L$  ( $x_D=1$ ) we can rewrite Eq. 1 as

$$C = \frac{1}{2} \operatorname{erfc} \left( \frac{1 - Q_D}{2\sqrt{Q_D/N_{Pe}}} \right) + \frac{e^{N_{Pe}}}{2} \operatorname{erfc} \left( \frac{1 + Q_D}{2\sqrt{Q_D/N_{Pe}}} \right) \dots\dots\dots (3)$$

or the more familiar simplified CD equation using only the first term,

$$C = \frac{1}{2} \operatorname{erfc} \left( \frac{1 - Q_D}{2\sqrt{Q_D/N_{Pe}}} \right) \dots\dots\dots (4)$$

which can be used for  $N_{Pe}>35$ . Perkins and Johnston give

$$K_l = D^* + \alpha u$$

$$K_t = D^* + \alpha_t u \dots\dots\dots (5)$$

where  $D^*=D_0/\tau$ ,  $D_0$  is molecular diffusion coefficient, the order of  $10^{-5}$  cm<sup>2</sup>/s for liquid-liquid systems, and  $\tau$  is tortuosity, about 1.5-2.

**Apparent Dispersivity.** Apparent dispersivity  $\alpha_a$  is determined by a best-fit match of the CD transport term to effluent profile  $C$  vs  $Q_D$  data from a field tracer test or numerical simulation. Most often the 1D CD equation is used directly to fit  $C(Q_D)$  data, where apparent Peclet number  $N_{Pea}$  is the fitting parameter,  $\alpha_a=L/N_{Pea}$ . Alternatively, a numerical model allows modification of the CD transport term to history match concentration profiles.

**Best Fit Procedure.** Our approach to fitting the CD Eq. 3 to effluent profiles minimizes a least squares function  $f$ ,

$$f(N_{Pe}) = \sum \Delta C_i^2 \dots\dots\dots (6)$$

$\Delta C_i$  is a residual defined as the difference in CD-model  $C$  and the  $C$  “data” being fit. Usually all data are fit, but sometimes data for only a limited range of  $Q_D$ .

The only model parameter is Peclet number  $N_{Pe}$ . The  $\alpha_a$  must be calculated from the best-fit  $N_{Pea}$  ( $=L/\alpha_a$ ) using scale  $L$  equal to “distance traveled”. For a transmission (two-well) test  $L$  is interwell distance.

For an echo (single-well) test  $L$  is twice the mean depth of penetration  $L_m$ <sup>12</sup>. For an  $x$ - $z$  cross-section  $L_m$  is calculated from  $qt=\phi_w H L_m$  where  $q$  is injection rate and  $t$  is time at the end of injection. For the field echo test,  $L_m$  is calculated from  $qt=\pi\phi H L_m^2$ .

**Conformance.** Conformance is usually considered to consist of two components – areal sweep and vertical sweep. Muskat<sup>14</sup> shows analytically that the two components of sweep can be treated individually and composited thereafter. Conformance reflects the combined effects of heterogeneity, well areal pattern and completion intervals, and drift.

**Well Pattern Areal Sweep.** Areal conformance is dictated by well placement in an areal pattern. Analytical solutions exist for the homogeneous 5-spot and 2-spot patterns. The confined 5-spot solution<sup>15</sup> is

$$Q_D = 0.457K(90C) \dots\dots\dots (7)$$

where  $K(x)$  is the complete elliptic integral of the first kind with  $x$  in degrees. Breakthrough time for the five-spot is  $Q_{DBT}=0.7178$ .

The unconfined 2-spot solution<sup>16</sup> is

$$Q_D = \frac{1 - \pi C / \tan(\pi C)}{\sin^2(\pi C)} \dots\dots\dots (8)$$

where pore volume is defined as  $\phi\pi H d^2$  and  $d$  is the distance between wells. Breakthrough occurs at  $Q_{DBT}=1/3$ .

**Stratification.** A *stratified* formation is defined as one where permeability varies only with  $z$ . Examples are the linear,

exponential, and log-normal  $k(z)$  described by Muskat<sup>14</sup>. Also, discrete layers of different permeabilities and thicknesses represent a stratified formation. If formation thickness is constant and wells are fully penetrating, there is no crossflow (vertical flow between layers) in a stratified formation and vertical permeability is irrelevant.

The Muskat model for exponential  $k(z)$  is given by

$$k(z) = k_{min} e^{bz/H} \dots\dots\dots (9)$$

where  $k_{max}=k_{min}e^b$ . Muskat further defines the ratio  $r=k_{max}/k_{min}$ . The Muskat model for linear  $k(z)$  is given by

$$k(z) = k_{min} [1 + (r - 1)z / H] \dots\dots\dots (10)$$

where again,  $r= k_{max}/k_{min}$ . The log-normal distribution of  $k(z)$ , as given by Muskat, is

$$dz / d\Psi = \frac{H}{\sigma\sqrt{2\pi}} e^{-\Psi^2 / 2\sigma^2} \dots\dots\dots (11)$$

where  $\Psi=\ln(k/k_{min})$ .

The Dykstra-Parsons  $V$  parameter is related to the log-normal standard deviation  $\sigma$  by the relation  $\sigma=-\ln(1-V)$ , or  $V=1-e^{-\sigma}$ .

**Heterogeneity.** Heterogeneity indicates spatial variation in rock properties, mainly permeability  $k(x,y,z)$  and porosity. Homogeneity, the opposite, implies uniform or spatially-invariant rock properties. *Stratification* is an example of heterogeneity in the  $z$ -direction with homogeneity in the  $x$ - and  $y$ -directions,  $k=k(z)$ .

**Muskat Analytical Model.** In 1949 Muskat<sup>14</sup> gave an analytical solution for the effect of any stratification  $k(z)$  on effluent profile  $C(Q_D)$ , for any areal geometry and well pattern with no vertical crossflow and negligible transverse dispersion. His solution is useful in examining and explaining the magnitude and scale-dependence of apparent dispersivities derived from tracer tests. Let the base function  $F$  be defined as the concentration profile response for a vertically-homogeneous system. His analytical solution is

$$C(Q_D) = \frac{\int_0^H F(Q_{Dz}) k(z) dz}{\bar{k} H} \dots\dots\dots (12)$$

where

$$Q_{Dz} = \frac{k(z)}{\bar{k}} Q_D \dots\dots\dots (13)$$

$$\bar{k} = \frac{\int_0^H k(z) dz}{H} \dots\dots\dots (14)$$

and  $F$  is any function giving concentration vs pore volumes injected for the vertically-homogeneous system. Example base functions  $F(Q_D)$  are the analytical five-spot<sup>15</sup> and two-spot<sup>16</sup> solutions ( $\alpha=0$ ), the step function from 0 to 1 at  $Q_D=1$  for the linear drive (100% areal conformance) with  $\alpha=0$ , and the CD

Eq. 3 for the linear drive with any  $\alpha > 0$ . Analytical  $F(Q_D)$  solutions are not available for areal well patterns including longitudinal physical dispersion. If such solutions can be determined by other means then they can be used in Eq. 12.

Muskat gives analytical integrations of his Eq. 12 for the exponential, linear, and log-normal probability stratifications  $k(z)$  of Eqs. 9-11 above. He shows that  $C(Q_D)$  is dependent only upon the single parameter  $r = k_{max}/k_{min}$  for the exponential and linear  $k(z)$  and only upon  $V$  for the log-normal  $k(z)$ . The  $k(z)$  function can be continuous or a step function representing any number of layers of any permeabilities and thicknesses. The ordering of  $k(z)$  is irrelevant. For the three  $k(z)$  stratifications just mentioned, and for any given  $k(z_D)$ ,  $C(Q_D)$  is independent of both  $H$  and scale  $L$  if  $\alpha = 0$ . Muskat notes that the linear  $k(z)$  case may be a reasonable approximation in some cases if permeabilities from logs and coreplugs are rearranged in monotonically increasing order.

**Single-Well “Echo” Test.** A single-well test, also referred to as an “echo” test, involves the injection of a tracer with constant concentration into a single well, followed by production from the same well. Well effluent concentrations are measured during the production period.

Traditional interpretation of an echo test uses the linear or radial CD equation, neglecting any regional flow field that might exist during the test. The radial CD equation proposed by Gelhar and Collins<sup>17</sup> can be shown to be “equivalent” to the simplified 1-term linear CD Eq. 4 for linear-model Peclet number  $N_{PeL} > 20$ , if we use the relation  $N_{PeL} = 6N_{PeR}$ , where  $N_{PeR} = L/\alpha$  and  $L = 2L_m$ .

**Two-Well “Transmission” Test.** A two-well test, also referred to as a “transmission” test, involves the continuous or slug injection of a tracer into one well, with production from a second well. Effluent concentrations are measured from the production well. In a *recirculating* two-well test, a tracer slug is injected followed by injection of produced water containing its tracer concentrations.

**Drift (Regional Flow Gradient).** In practically all groundwater systems and in petroleum reservoirs with an active flood, a regional flow gradient (“drift”) exists where the tracer test is conducted<sup>18,19</sup>. Interference of the natural linear velocity field and the test well radial velocity field changes the otherwise circular shape of the injected tracer front to a distorted ellipse. For an echo test, the resulting smeared effluent profile will have an associated apparent dispersivity  $\alpha_a > \alpha$ . Most references in the literature tend to ignore the effect of drift on test results.

We present simulation results that indicate drift provides a physical explanation for large apparent dispersivities reported for the single- and two-well tests of Pickens and Grisak.<sup>12</sup>

**Numerical Modeling Well Effluent Concentrations.** In this study we used three numerical models: (1) Sensor<sup>20</sup>, a finite-difference simulator using single-point upstream weighting; (2) UTCHEM<sup>21</sup>, a finite-difference simulator using TVD higher-order difference scheme; and (3) 3DSL<sup>22</sup>, a streamline simulator.

## Heterogeneity Alone Causes No In-Situ Mixing

Heterogeneity alone ( $\alpha = \alpha_r = D_0 = 0$ ) causes no in-situ mixing. For  $\alpha = \alpha_r = D_0 = 0$ , the transport equation is hyperbolic, containing first-order terms  $u_x \partial C / \partial x$ ,  $u_y \partial C / \partial y$ ,  $u_z \partial C / \partial z$  but no second-order terms. As a consequence, the displacement front is piston-like with no transition zone.

To illustrate, consider a 2D heterogeneous 5-spot with a 7x7 checkerboard description. The red squares (on the diagonals) are 100 md and 0.2 porosity and the black squares are 1 md and 0.1 porosity. Fig. 1 shows a concentration contour map at 0.3366 pore volumes injected, calculated using the 3DSL streamline model with a 567x567 grid and 3688 streamlines. The displacement front is piston-like; there are no concentrations between 0 and 1.

The effluent profile shown in Fig. 2 is, however, smeared, reflecting conformance caused by the severe heterogeneity. The system has an apparent Peclet number of 2.7 (poor-quality fit), with an apparent dispersivity  $\alpha_a = L/2.71$ . This  $\alpha_a$  is a “conformance index” bearing no relation to mixing in the reservoir. The Peclet number of 2.71 compares with an apparent Peclet number of 18 for the homogeneous 5-spot case. On a log-log plot of  $\alpha_a$  vs scale  $L$ , both this heterogeneous case and the homogeneous case exhibit scale-dependent (parallel) lines of slope 1, but the heterogeneous  $\alpha_a$  values are about 7 times larger at any  $L$ . Recall that physical dispersivity  $\alpha$  is zero for both of these cases.

Heterogeneity alone causes smeared effluent curves and large, scale-dependent apparent dispersivities. But it does not cause in-situ mixing.

Single-well tracer tests give echo apparent dispersivities up to 3 ft or larger<sup>6,12</sup>. Several authors state these echo apparent dispersivities should approximate physical dispersivity in stratified formations where crossflow is absent<sup>2,6,12</sup>. This should also be true in formations of arbitrary heterogeneity with crossflow if drift is zero or negligible. For zero physical dispersivity, a streamline model will calculate a diverging piston-like displacement front during injection. The streamlines do not change with time and the shape of the front will reflect the formation heterogeneity. Upon initiation of production, all points on the displacement front will retreat toward the well, arriving at the same time, giving a step-function effluent profile. Thus, heterogeneity alone (of any type, in the absence of drift) cannot be considered the reason for observed apparent echo dispersivities 10 to 100 or more times larger than lab-measured  $\alpha \sim 0.01$  ft.

## Scale Dependence of Apparent Dispersivity

Plots of apparent dispersivity versus scale<sup>1,2</sup> (travel length)  $L$  show a near linear dependence, though scatter is significant. An acceptable explanation for this linear scale dependence is not readily found in the literature. Physical dispersion associated with in-situ mixing is known to be invariant with travel distance, so the explanation must lie elsewhere.

In this paper we show that the scale dependence of apparent dispersivity, when it exists, is a *natural and expected* consequence of the fact that apparent dispersivities reflect conformance – *not* physical dispersion.

**Five-Spot.** We start with the simple example of a homogeneous five-spot. The analytical solution Eq. 7 gives a unique function  $C(Q_D)$ . A fit of this profile to the CD Eq. 3 gives a best-fit (for  $0 < Q_D < 2$ ) apparent conformance Peclet number of  $N_{Pea} = N_{Peap} = 18$ . This corresponds to a scale-dependent apparent dispersivity of

$$\alpha_a = \frac{1}{N_{Pea}} L = \frac{1}{18} L = 0.056L$$

Fig. 3 shows the best-fit of this solution. Fig. 4 shows the resulting plot of  $\alpha_a$  versus  $L$ , superimposed on literature-reported apparent dispersivities.

**Two-Spot.** Next we consider a homogeneous two-spot. The analytical solution Eq. 8 gives a unique function  $C(Q_D)$ . A fit of this profile to the CD Eq. 3 gives a best-fit (for  $0 < Q_D < 2$ ) apparent conformance Peclet number of  $N_{Pea} = N_{Peap} = 3$ . This corresponds to a scale-dependent apparent dispersivity of

$$\alpha_a = \frac{1}{3} L = 0.33L$$

Fig. 3 shows the best-fit of this solution. The fit is not good for  $Q_D > 0.8$ , and increasingly poor for  $Q_D > 1$ ; depending on the range of  $Q_D$ , the best-fit apparent Peclet number will vary. Fig. 4 shows the resulting plot of  $\alpha_a$  versus  $L$  for a 2-spot with  $N_{Pea} = 3$ .

The two-spot solution is the *expected* performance of a two-well transmission test (in the absence of drift). Some authors correctly interpret transmission profiles with a 2-spot flow model<sup>12</sup>, but still require apparent dispersivities to match field data affected by other conformance issues such as stratification and drift.

**Stratification.** Now we consider the case of stratification only (100% areal conformance), using various  $k(z)$ . For a given  $k(z)$ , the Muskat Eq. 12 gives a unique  $C(Q_D)$ , using the step function for  $F(Q_D)$ . For example, using the log-normal  $k(z)$ <sup>14</sup> and  $V = 0.5$  gives the result in Fig. 5. A fit of this profile to the CD Eq. 3 (for  $0 < Q_D < 4$ ) gives an excellent best-fit apparent Peclet number of  $N_{Pea} = N_{Peas} = 3.5$ . This corresponds to a scale-dependent apparent dispersivity for  $V = 0.5$ ,

$$\alpha_a = \frac{1}{3.5} L = 0.286L$$

Fig. 6 shows the  $\alpha_a$  versus  $L$  relationship for a number of values for three apparent Peclet numbers: 5, 50, and 500, superimposed on literature-reported  $\alpha_a$  for a wide range of single- and two-well test data. This range of  $N_{Pea}$  brackets practically all of the reported apparent dispersivities from field test data. Fig. 7 shows a plot of  $N_{Pea}$  versus  $V$  (red line). An approximate relation for  $N_{Pea}(V)$  was suggested by Warren and Skiba<sup>11</sup>,

$$N_{Pea} \approx 2 / (\ln(1 - V))^2 \dots\dots\dots (15)$$

which is accurate for  $V < 0.4$ , but increasing overpredicts  $N_{Pea}$  at  $V > 0.4$  (e.g. estimated  $N_{Pea} = 0.77$  at  $V = 0.8$  vs the “correct” CD best-fit value of  $N_{Pea} = 0.3$ ).

A similar analysis was performed for the Muskat linear and exponential  $k(z)$  stratification. Results are shown in Fig. 7 (blue and pink lines, respectively).

For further discussion of the black circles and line on Fig. 7, see the section *Additive Conformance Dispersivities* at the end of the Appendix.

**Stratified Five-Spot.** Let us consider the case of a stratified five-spot system. The Muskat solution Eq. 12 is used to calculate  $C(Q_D)$ , using  $F(Q_D)$  given by the 5-spot solution Eq. 7 and the log normal  $k(z)$  with  $V = 0.353$ . Fig. 8 shows  $C(Q_D)$  and a near-exact CD Eq. 3 best-fit with apparent Peclet number  $N_{Pea} = 6$ .

Best-fit  $N_{Peas} = 10$  for  $V = 0.353$  stratification alone. Best-fit  $N_{Peap} = 18$  for a 5-spot pattern alone. Using additive dispersivities (see Appendix), this 5-spot stratified system has an effective Peclet number  $N_{Pea} \approx 1 / (1/18 + 1/10) = 6.4$ , quite close to the best-fit value of 6.

**The Linearity and Scatter of  $\alpha_a$  Scale Dependence.** We call two purely convective ( $\alpha = 0$ ) systems of different scale  $L$  *similar* if their descriptions in terms of  $x_D, y_D, z_D$  are identical. A precise definition of similar systems is difficult, so we simply proceed with illustrative examples.

Five-spots of different scale  $L$  with the same stratification<sup>c</sup> in the absence of drift are similar systems. Every such system has the same effluent profile  $C(Q_D)$  and the same best-fit Peclet number. The apparent dispersivities will plot exactly as a straight line of slope 1 on a log-log plot of  $\alpha_a$  vs  $L$ . The same can be said for two-spots of different scale  $L$  with the same stratification. Such similar systems will always give a straight line of slope 1 on a log-log plot of  $\alpha_a$  vs  $L$ , with the intercept determined by its apparent Peclet number. The resulting log-log plot will exhibit a general trend of  $\alpha_a$  increasing with  $L$  with a slope of 1, but, clearly, with considerable scatter.

**Example of Similar Systems.** An example of a similar system is a confined 5-spot. with stratification  $k(z)$  given by  $V = 0.353$ . Pattern areas of 5-acres, 10-acres, and 40-acres will have the same  $C(Q_D)$  profiles. Muskat’s  $C(Q_D)$  solution for this system is shown in Fig. 8, with a best fit Peclet number of 6. The  $\alpha_a$  for this system will plot as a straight line of slope 1 on a log-log plot of  $\alpha_a$  vs  $L$ . With interwell distances of  $L = 330, 467,$  and  $933$  ft for the 5-, 10-, and 40-acre patterns, respectively,  $\alpha_a = (330/6) = 55$  ft for the 5-acre pattern;  $\alpha_a = (467/6) = 78$  ft for the 10-acre pattern; and  $\alpha_a = (933/6) = 155$  ft for the 40-acre pattern.

An example of approximately similar systems is shown in Fig. 9. Three reservoirs with different stratification  $k(z)$  descriptions were chosen:  $V = 0.353$ , linear  $r = 5.49$ , and exponential  $r = 3.95$ . Areal conformance is taken as 100%. The  $C(Q_D)$  solutions from the Muskat Eq. 12 solution for each reservoir are shown as solid lines in Fig. 9. Slight differences in profiles are seen for the different stratifications, but each one is described by the same best-fit apparent Peclet number

<sup>c</sup> *Same stratification* means the same value of  $r = k_{max}/k_{min}$  or  $V$  for the three Muskat  $k(z)$  models; or, for other  $k(z)$ , the same  $k(z_D)$ , remembering that the ordering of  $k$  is irrelevant.

of 10 using the 1D CD equation. Therefore the three systems are considered *approximately similar*.

**A System without  $\alpha_a$  Scale Dependence.** Consider an echo test with drift. The  $\alpha_a$  scale dependence becomes complicated, if not void of meaning. The distance traveled  $L$  is  $2L_m$  where  $L_m^2 = Q_{inj}/\pi H\phi$ . But  $Q_{inj} = qt$  for a constant injection rate, which gives an infinite number of combinations of  $q$  and  $t$  (time at the end of injection) with the same  $Q_{inj}$  and, therefore, with the same  $L$ . For a fixed  $L$ , however, every valid combination of  $q$  and  $t$  results in a *different*  $C(Q_D)$  relation, with *different* apparent dispersivities. This will obviously lead to scatter, potentially severe, as shown in a later example. Furthermore, if two tests are run, each with a different  $L$ , the resulting apparent dispersivity can literally have any slope on a log-log plot of  $\alpha_a$  vs  $L$ : 0,  $\infty$ , -1 or (fortuitously) 1.

The problems just described are illustrated, based on 3D Sensor simulations made of the Pickens-Grisak single-well test area. After having matched the two SW1 and SW2 echo tests with a model correctly describing the field-observed drift, a number of echo-test simulations were made at two rates with varying injection periods. Table 1 gives results of the simulated tests, with best-fit apparent dispersivities for each test. If we choose randomly any two of the tests to define the system scale dependence, the resulting slope on a log-log plot of  $\alpha_a$  vs  $L$  will range from 0 to  $\pm\infty$ . Halving the rate and doubling the injection period to maintain a *constant*  $L$  results in an apparent dispersivity increase by a factor of 3 to 4 (i.e. severe “scatter”). For a fixed injection rate and varying injection period, the slope is approximately 2, but varying somewhat. See the section *SW1 & SW2 Echo Tests Including Drift* below for further discussion.

## Field and Laboratory Examples

**Greenkorn Laboratory Five-Spot.** This problem is a laboratory quarter 5-spot tracer test reported by Greenkorn et al<sup>23</sup>. They conducted confined 5-spot miscible flood field tests for mobility ratios of 1, 0.1 (favorable), and 10 (unfavorable). A layered 22.3 in. x 22.3 in. x 6.7 in. quarter 5-spot lab model was constructed, scaled by a factor of 13.33 from their 50 ft x 50 ft x 8.4 ft field (full) 5-spot pilot. Thicknesses and permeabilities of the three layers in their lab model were calculated by scaling criteria from extensive field core permeability data and are given in Table 2.

Fig. 10 compares observed recovery of displaced fluid for  $M=1.0$  with that calculated from the Muskat Eq. 12 using the 5-spot analytical  $F=C(Q_D)$  relation (Eq. 7) and layer properties in Table 2. The close agreement indicates that areal and vertical conformance dominate the effluent profile, while physical dispersion effects in the lab model were negligible. Physical dispersion effects should be even lower at field scale because conformance-based apparent dispersivity increases linearly with length, while physical dispersivity is a constant and small value compared with  $\alpha_a$ .

We calculated an apparent Peclet number  $L/\alpha_a$  of 16.25 from the best fit of Eq. 3 to the  $C(Q_D)$  result from the Muskat solution, as shown in Fig. 11. This solution is scale-independent. The corresponding apparent dispersivity is  $\alpha_a = 0.0615L$ , or 0.665 m for the field test using  $L =$  interwell distance = 10.8 m, and assuming equivalent field and lab

model descriptions. The apparent dispersivity from the lab model is 13.3 times less, or 0.05 m. The field scale apparent dispersivity of 0.665 m at a scale  $L$  of 10.8 m can be noted on Fig. 6 and agrees well with the field data points. Note that (a) this 0.665 m apparent dispersivity is more than 200 times larger than a lab-measured dispersivity of  $\sim 0.01$  ft, and (b) the Muskat analytical solution closely matching the lab test data (Fig. 10) has no dispersion and no in-situ mixing.

**Pickens-Grisak<sup>12</sup> Echo Tests.** The single-well echo tests presented by Pickens and Grisak in 1981 are studied below. These authors provide detailed information about a groundwater system and two echo tests conducted in a single well. They fit the production profiles to a radial 1D CD equation essentially equivalent to the simplified one-term linear 1D CD Eq. 4

**SW1 Echo Test.** Apparent dispersivity of  $\alpha_a=3$  cm was reported for SW1. Travel distance was  $L=2L_m=6.26$  m. Results are given in terms of a  $Q_p/Q_{inj}$  ratio which is related to  $Q_D$  by  $Q_p/Q_{inj}=1+2(Q_D-1)$ , or  $Q_D=0.5(Q_p/Q_{inj}+1)$ . Our fit of their observed profile to the linear CD Eq. 3 gives the same  $\alpha_a = 3$  cm, as shown in Fig. 12.

Pickens and Grisak do not give a quantitative model to explain an apparent dispersivity some 85 times their lab-measured physical dispersivity of 0.035 cm (0.00115 ft).

**SW2 Echo Test.** Apparent dispersivity of  $\alpha_a=9$  cm was reported for SW2. Travel distance was  $L=2L_m=10$  m. Our fit of their observed profile to the linear CD Eq. 3 gives basically the same  $\alpha_a=8.5$  cm, as shown in Fig. 13.

Pickens and Grisak do not give a quantitative model to explain an apparent dispersivity some 250 times their lab-measured physical dispersivity of 0.035 cm (0.00115 ft).

**SW1 & SW2 Echo Tests Including Drift.** Pickens and Grisak state that “the effect of natural regional flow is generally assumed to be negligible in the vicinity of the two wells” (one of the wells being that used in SW1 and SW2). However, the authors do provide detailed field data quantifying the regional groundwater flow gradient (drift). Our interpretation of their Fig. 2 gives 0.0023 psi/ft at the location of the single- and two-well tests (Fig. 14).

We conducted a numerical model study with Sensor using an  $r-\theta$  simulation of a single layer with 2810 ft diameter, with the test well at its center. Data were taken from the Pickens and Grisak SW2 test. Porosity was 0.38, permeability was 14.8 D (from their Eq. 24). The test well injection and production rates were 14.5 and 12.22 RB/D/ft of thickness. Injection and production times were 3.93 and 9.326 days, respectively.

A 1000x25  $r-\theta$  grid was used to represent the symmetrical half-circle. The radial spacing was 999 equal-volume blocks from  $r=r_w=0.17$  ft to  $r=20$  ft and one block from  $r=20$  to  $r=1405$  ft. Angular spacing was uniform with  $\Delta\theta=7.2^\circ$ . Injection and production wells in cells (1000,25) and (1000,1), respectively, operated on pressure constraint, to give a nearly uniform linear velocity gradient of  $\sim 0.0023$  psi/ft within the 40 ft diameter of the test well region.

We made various simulations to evaluate numerical dispersion. For a zero hydraulic gradient, the radial spacing combined with running at the stable step (CFL=1) gave zero

numerical dispersion as shown by the step-function on Fig. 15. Including the hydraulic gradient, numerical dispersion has a negligible effect on the calculated effluent curve, as grids of 500x25 and 1000x50 gave identical results (Fig. 15).

The resulting model comparison with test data is shown in Fig. 15, with what we consider to be an excellent match. Recall that the simulation results are based solely on a geological layer description including measured drift – i.e., predictive and with no physical dispersion.

Fitting the model results with the CD equation we get a best-fit apparent dispersivity of 11 cm, similar to the 9 cm found when fitting the data themselves.

We also simulated the SW1 test with drift. The finely-gridded well test area was a circle of diameter 23 ft. Injection and production rates were 17.868 RB/D/ft. Injection and production times were 1.25 and 2 days, respectively. Fig. 16 compares observed and calculated results (for 1000x25 grid) effluent profiles, again with a good match.

The best-fit apparent dispersivity to our model profile is 1.6 cm, compared with 3 cm when fit to the data directly.

We repeated the above Sensor  $r$ - $\theta$  runs with  $r$ - $\theta$ - $z$  runs using the layered  $k(z)$  description tabulated by Pickens and Grisak. These runs showed very little effect of the stratification.

Having a predictive model to describe the well used for SW1 and SW2 tests, we ran a number of simulations to study the relation of apparent dispersivity to travel distance ( $2L_m$ ). A constant rate test was simulated for varying injection periods: 1, 3, 4.5, 6, and 8 day runs for each rate. The first rate was the same as used in SW1, 17.868 RB/D/ft, and the second series of simulations used a rate one half that value. Results are shown in Table 1 and Fig. 17, and they are discussed in the previous section *A System without  $\alpha_a$  Scale Dependence*. Fig. 18 illustrates how two echo tests with identical length scales of 9.7 m have dramatically different  $C(Q_D)$  profiles because of drift.

**SW2 Echo Test Modeling with Lamination and Physical Transverse Dispersion.** Pickens and Grisak note that transverse dispersion between layers may give apparent echo dispersivity larger than physical dispersivity. They reported laminations 0.1-0.5 cm thick, textural variations over several to tens of cm, and an 18-layer (each 45 cm thick)  $k(z)$  description, but gave no estimate of adjacent sublayer or lamination permeability contrasts.

A Sensor simulation of the echo test SW2 was built using a description of alternating layers of thickness  $h$ , a permeability ratio 3:1, with no drift. The symmetrical element is two adjacent layers, each of thickness  $h/2$ . The 2D  $r$ - $z$  CD equation was solved with longitudinal  $K_f=0$  and  $K_r=D^*+\alpha_r u(z)$  using a computational  $r$ - $z$  grid of 1000x8. The radial spacing corresponded to equal-volume grid blocks between  $r=r_w=0.17$  ft and outer radius  $r_e=22$  ft. This spacing and use of the maximum stable step minimized numerical dispersion. Numerical dispersion was determined from a run with  $K_f=0$ . The SW2 rate of 14.5 RB/D/ft and injection time of 3.93 days were used. Effective molecular diffusion  $D^*$  was 0.001 ft<sup>2</sup>/d corresponding to a liquid-liquid molecular diffusion coefficient of about  $2 \cdot 10^{-5}$  cm<sup>2</sup>/sec and a tortuosity of 2. Transverse dispersivity was 0.0035 cm (ten times less than the lab-measured  $\alpha$  of 0.035 cm).

Fig. 19 compares observed and model  $C$  vs  $Q_p/Q_{inj}$  for layer thickness = 0.08 ft (2.44 cm). The best fit apparent dispersivity  $\alpha_a$  for the model effluent curve is 11 cm. We estimate that numerical dispersion contributed <2% of that value. The simulation used withdrawal rate equal to injection rate whereas the test withdrawal rate was actually somewhat less than injection rate. The description used is simplistic relative to the many possible variable-permutations and depth-dependent variations in those permutations; the results nevertheless indicate that transverse dispersion can give apparent echo dispersivities two to three orders of magnitude larger than lab-measured values. Note that there is no crossflow in this problem – i.e. vertical permeability is irrelevant.

We have stated earlier that heterogeneity alone causes no in-situ mixing. Here there is in-situ mixing *and* heterogeneity. But this mixing is *caused* by flow with transverse dispersivity  $\alpha_t > 0$ . The level of heterogeneity affects the *amount* of mixing *caused by flow with  $\alpha_t > 0$*  but the heterogeneity does not *cause* the mixing. Heterogeneity alone ( $\alpha = \alpha_t = D_0 = 0$ ) causes no in-situ mixing. If  $\alpha_t$  were 0 in the heterogeneous case of this section, there would be no in-situ mixing.

**Pickens-Grisak Two-Well Test.** This is a 15-day recirculating two-well tracer test with an interwell distance of 8 m reported by Pickens and Grisak. Fig. 20 (their Fig. 14) compares their observed effluent profile with the calculated profile from a single-layer 2-spot numerical model proposed by Grove<sup>12</sup> with an apparent dispersivity  $\alpha_a=50$  cm.

A Sensor run was made using a 1000x25x6  $r$ - $\theta$ - $z$  ( $i,j,k$ ) grid, with the producer at the center, for the symmetrical half-circle. The grid used 999 equal-volume radial gridblocks between  $r=r_w=0.17$  ft and  $r=40$  ft,  $r_e=1405$  ft, and uniform angular spacing  $\Delta\theta=7.2^\circ$ . Injection and production wells at (1000,25) and (1000,1), respectively, were operated on pressure constraint to give a nearly uniform linear drift gradient of 0.0023 psi/ft in the 80 ft diameter test area. The test injection well was located at  $j=25$ , 8 m upstream (relative to drift) from the producer. All wells were completed in all 6 layers. Numerical dispersion was found to be very low by comparing a single-layer Sensor run with no drift to the analytical two-spot solution Eq. 8. The 6-layer description used is a good approximation to the 18-layer description tabulated by Pickens and Grisak.

The first Sensor run used injected concentration equal to internally calculated produced concentration after 3.22 days, representing recirculation. Fig. 20 shows the Sensor results (red curve).

Fig. 20 also shows measured concentrations for the production well (gray circles) and for the injection well (black circles)<sup>25</sup> We have no explanation for the difference between concentrations measured from the same stream at the production well and the injection well, other than data uncertainty.

A second Sensor run was made using the reported injection concentration profile for  $t > 3.22$  days (black circles in Fig. 20), resulting in the calculated effluent profile shown in Fig. 20 (black line).

Both Sensor predictions, based on field-measured reservoir description (stratification and drift), predict effluent profiles consistent with measured (a) breakthrough time, 3 days, (b) time of maximum concentration, ~7 days, (c) maximum concentration 0.21-0.27, and (d) “flattening” concentration level of ~0.2 for  $t > 10$  days. Given that this same reservoir description, with zero input physical dispersion, also predicts accurately the SW1 and SW2 single-well tests at the same well location, we suggest that the test area conformance is adequately history-matched by modeling stratification and drift only, without the need for apparent dispersivity.

Areal heterogeneity and/or different layered descriptions were not explored, these factors possibly helping to fine-tune the history match.

### Modeling Examples

**Mahadevan et al.<sup>2</sup>** This paper presents a number of simulation studies conducted to provide understanding of apparent dispersivities. We discuss several issues brought forth in that paper, and a somewhat different interpretation of results presented therein.

**Five-Layer Problem.** Their example is a 30 ft x 20 ft layered  $x$ - $z$  cross-section used to numerically simulate a two-well field tracer test using a 30x5  $xz$  grid. Layer permeabilities are 200, 500, 800, 1100, and 1400 md, each 4-ft thick. One pore volume is 72.66 RB. They used large input dispersivities  $\alpha = 0.46$  m and  $\alpha_i = 0.046$  m ( $\alpha_i$  has no effect<sup>24</sup>). Crossflow does not exist so vertical permeability is irrelevant.

The analytical solution for the transmission effluent curve is given by Muskat’s Eq. 12 using the base function  $F$  from Eq. 3. Fig. 21 shows the Muskat analytical solutions for input  $\alpha = 0$ , and for input  $\alpha = 0.46$  m. Mahadevan et al’s simulated effluent profile (for input  $\alpha = 0.46$  m) is in exact agreement with the Muskat solution shown in Fig. 21.

The Muskat effluent profiles yield best-fit apparent dispersivities of 1.63 m and 2.24 m for  $\alpha = 0$  and  $\alpha = 0.46$  m, respectively. This  $\alpha_a = 2.24$  m is roughly equal to the sum of conformance and input (“physical”) dispersivities,  $\alpha_a = \alpha_{ac} + \alpha$  ( $= 1.63 + 0.46$ ), additive dispersivity Eq. A-1.

For zero input  $\alpha$ , the Muskat analytical solution gives  $\alpha_a = 1.63$  m and reflects no mixing in the reservoir. This large  $\alpha_a$  reflects only conformance of the layer heterogeneity, and is >500 times larger than a typical lab-measured physical  $\alpha \sim 0.01$  ft. Fig. 22 shows the accuracy of the UTCHEM solution for input  $\alpha = 0$ , compared with the Muskat analytical solution.

The Muskat  $C$  profile for  $\alpha = 0$  and its best-fit Peclet number ( $N_{pea} = L/\alpha_a = 5.61$ ) is scale-independent (independent of  $L$  and  $H$ ). The scale dependence of  $\alpha_a = L/5.61$  is a meaningless consequence of applying the non-applicable CD Eq. 3 to a profile dominated by conformance.

**Eight-Layer Problem,  $k_v = 0$ .** This problem is an  $x$ - $z$  cross section with  $k_v = 0$ , eight 2.5-ft thick layers, and a stochastic permeability distribution. Mahadevan et al numerically simulated this system to obtain apparent dispersivities for two-well (transmission) and single-well (echo) tracer tests. They used  $N_x \times 8$  grids with a uniform cell size of 1 ft x 2.5 ft, and large input dispersivities of  $\alpha = 0.46$  m and  $\alpha_i = 0.046$  m.

This problem is the same type of problem as the five-layer problem discussed above – i.e., a layered 2D  $x$ - $z$  cross section

with no crossflow. The permeability  $k_j$  of layer  $j$  is the harmonic average  $k_j = (L/\Delta x) / \sum_i k_{ij}^{-1}$  where the summation is from  $i=1$  to  $N_x$ . Sensor numerical solutions show negligible effects of transverse dispersion for  $\alpha_i < 0.0046$  m, which is 15 times larger than a physical value ~0.001 ft. Therefore, Muskat’s Eq. 12 gives the analytical solution to this problem for  $\alpha_i < 0.0046$  m and any value of  $\alpha$ . The analytical effluent profiles give the following transmission apparent dispersivities  $\alpha_a$  (m):

Length $L$ (ft)	Apparent Dispersivities $\alpha_a$ (m) for Model	
	Input $\alpha = 0$	Input $\alpha = 0.46$ m
30	11.4	12.1
60	31.4	32.4
100	56.4	57.6

The large apparent dispersivities reflect only conformance and provide no support for large physical dispersivities. The additive dispersivity relation (Eq. A-1) becomes more approximate as  $L$  and  $\alpha_a$  increase.

**Eight-Layer Problem,  $k_v = k_h$ .** These simulations use  $k_v = k_h$ , for the same problem just described. Because crossflow exists the Muskat solution does not apply. Mahadevan et al numerically simulated this problem to obtain apparent transmission, echo, and local dispersivities (their Fig. 10). Again they use large input dispersivities  $\alpha = 0.46$  m and  $\alpha_i = 0.046$  m. Local dispersivities are those obtained from individual gridblock  $C(t)$  profiles.

Their reported local and echo dispersivities, and scale-dependence of the latter, reflect significant numerical dispersion. A simple way to check numerical dispersion levels is to perform simulations using zero input dispersivities. For the runs and results described here, we ran UTCHEM using their datasets. Fig. 23 shows individual cell  $C(t)$  profiles for the transmission case  $L = 60$  ft using zero input dispersivities. The profiles differ significantly from expected zero-dispersivity vertical step functions from 0 to 1. Best-fit local apparent dispersivities (using  $L = i$  ft,  $\Delta x$  was 1 ft) for these profiles shown range from 0.042 m to 0.952 m and reflect *only* numerical dispersion.

Using zero input dispersivities we ran UTCHEM echo tests for scale  $L = 22.06, 44.12,$  and  $80.88$  ft. Fig 24 shows the  $C$  profile for  $L = 80.88$  ft. The profile for input  $\alpha = \alpha_i = 0$  shows significant numerical dispersion (the correct profile is a step function from 1.0 to 0 at  $Q_D = 1.0$ ). Arguably, the correct profile for  $\alpha = 0.46$  m corresponds to Eq. 3, shown in Fig. 24. We believe numerical dispersion affects the apparent echo dispersivities (2 m at  $L = 80.88$  ft) and the scale dependence shown in their Fig. 10.

### Arbitrariness of Apparent Dispersivity.

In field tests the many factors comprising conformance strongly affect the observed produced effluent profiles. The approach to modeling effluent profiles may vary widely: (a) simple application of the CD Eq. 3, (b) single-layer models with proper areal sweep description, (c) models that treat both areal and vertical conformance (e.g. Muskat Eq. 12), or (d) 3D

numerical simulators that describe conformance and physical dispersion, but which may suffer from numerical dispersion.

Independent of which approach is used, if conformance is not handled accurately then a “correction term” is needed to match well effluent profiles. This often means the introduction of an apparent dispersivity. A problem with consistent use of apparent dispersivities (e.g. plots of  $\alpha_a$  versus  $L$ ) is that they are strongly dependent on the base model used (simple or detailed geologic description, accurate or approximate flow model, etc.). A simple model typically leads to a large  $\alpha_a$  while a more accurate model leads to lower  $\alpha_a$ . A “correct” model doesn’t require apparent dispersivity, and physical dispersivities, if included, usually have no impact.

The goal of any modeling study should be to build a model that eliminates the need for apparent dispersivities to match well effluent profiles. If apparent dispersivity is needed, then never use the history-matched value ( $\gg 0.01$  ft) in the physical CD flow terms describing phenomena such as miscible bank breakdown, in-situ scale precipitation or chemical reaction.

## Conclusions

1. Heterogeneity alone ( $\alpha = \alpha_r = D_0 = 0$ ) causes no in-situ mixing in the reservoir.
2. *Physical* dispersivity  $\alpha$  is a rock property the order of 0.01 ft for consolidated rocks and significantly smaller for unconsolidated sand packs. It is independent of time and scale, regardless of whether scale is defined as system length, distance traveled, or “scale of heterogeneity”.
3. *Apparent* dispersivity  $\alpha_a$  is obtained by matching observed or numerically calculated effluent concentration curves with the one-dimensional convection-dispersion (1D CD) equation. That equation does not physically describe field tracer test behavior. That behavior largely reflects areal and vertical conformance, which in turn depend upon well pattern and completion intervals, heterogeneity, and drift.
4. The observed *scale dependence* of apparent dispersivity is empty of meaning. When it exists then it is a necessary consequence of applying the non-applicable 1D CD equation with its single parameter, the Peclet number  $L/\alpha$ , to match effluent profiles reflecting conformance.
5. The *magnitude* of apparent dispersivity  $\alpha_a$  is predominately that due to conformance effects alone,  $\alpha_{ac}$ , corresponding to no physical dispersion or in-situ mixing ( $\alpha = 0$ ). In fact,  $\alpha_a$  is roughly the additive function  $\alpha_{ac} + \alpha$ , where  $\alpha_{ac} \gg \alpha$ .
6. Numerical simulations of any reservoir process of any mobility ratio – e.g. enriched gas drives, solvent floods, bank breakdown, tracer tests - should use physical dispersivities the order of 0.01 ft, not apparent dispersivities typically 100 to 1000 times larger.

## Acknowledgements

The authors would like to thank Marco Thiele for helping prepare the contour map in Fig. 1, and to Lee Chin and Ray Pierson for their assistance with the UTCHEM simulations.

## Nomenclature

- $b$  = parameter in Muskat exponential  $k(z)$  equation,  $= \ln(k_{max}/k_{min})$
- $C$  = concentration, fraction, normalized to 1.0 for initial injected tracer concentration
- $K_l$  = longitudinal dispersion coefficient,  $ft^2/s$  or  $cm^2/s$  [ $L^2/T$ ]
- $K_t$  = transverse dispersion coefficient,  $ft^2/s$  or  $cm^2/s$  [ $L^2/T$ ]
- $D^*$  = effective molecular diffusion within a porous media,  $cm^2/s$  [ $L^2/T$ ]
- $f$  = least squares function
- $F$  = function  $F(Q_D)$  describing the areal variation of concentration, used in Muskat’s analytical equation that composites areal and vertical conformance
- $h$  = layer thickness, ft or m [ $L$ ]
- $H$  = total formation thickness, ft or m [ $L$ ]
- $k$  = permeability, md [ $L^2$ ]
- $k_{ij}$  = permeability in cell  $i,j$ , md [ $L^2$ ]
- $k_j$  = permeability in layer  $j$ , md [ $L^2$ ]
- $k_v$  = vertical permeability, md [ $L^2$ ]
- $K$  = elliptic integral of first kind
- $L$  = travel distance or length, ft or m [ $L$ ]
- $L_m$  = mean depth of penetration in echo test, ft or m [ $L$ ]
- $M$  = mobility ratio
- $N_{Pe}$  = Peclet number, dimensionless
- $N_{Pea}$  = apparent Peclet number, dimensionless
- $N_{Peac}$  = apparent Peclet number due only to conformance, dimensionless
- $N_{Peap}$  = apparent Peclet number due only to areal conformance, dimensionless
- $N_{Peas}$  = apparent Peclet number due only to stratification (vertical) conformance, dimensionless
- $N_{PeL}$  = Peclet number in linear CD equation, dimensionless
- $N_{PeR}$  = Peclet number in radial CD equation<sup>17</sup>, dimensionless
- $q$  = volumetric rate (=injection rate), bbl/d or  $m^3/d$  [ $L^3/T$ ]
- $Q_D$  = pore volumes injected, dimensionless
- $Q_{DBT}$  = pore volumes injected at breakthrough, dimensionless
- $Q_{Dz}$  = pore volumes injected into a given layer  $z$ , dimensionless
- $Q_{inj}$  = total volume injected in an echo test,  $ft^3$  or  $m^3$  [ $L^3$ ]
- $Q_p$  = volume produced in an echo test,  $ft^3$  or  $m^3$  [ $L^3$ ]
- $r$  = parameter in Muskat  $k(z)$  equations,  $= k_{max}/k_{min}$
- $r_w$  = wellbore radius, ft or m [ $L$ ]
- $r_e$  = external boundary radius, ft or m [ $L$ ]
- $t$  = time [ $T$ ]
- $u$  = pore velocity, ft/d or m/d [ $L/T$ ]
- $\Delta x$  = grid cell width, ft or m [ $L$ ]
- $x, y, z$  = Cartesian coordinates, ft or m ( $L$ )
- $x_D, y_D, z_D$  = dimensionless coordinates,  $x/L, y/w, z/H$
- $V$  = parameter in Dykstra-Parsons  $k(z)$  log-normal distribution =  $1 - e^{-\sigma}$
- $w$  = width, ft or m [ $L$ ]

- $z$  = vertical depth, ft or m [L]  
 $z_D = z/H$ , dimensionless  
 $\alpha$  = physical (longitudinal) dispersivity, ft or m [L]  
 $\alpha_t$  = physical transverse dispersivity, ft or m [L]  
 $\alpha_a$  = apparent physical dispersivity, ft or m [L]  
 $\alpha_{ac}$  = apparent physical dispersivity due only to conformance, ft or m [L]  
 $\alpha_{ap}$  = apparent physical dispersivity due only to areal conformance, ft or m [L]  
 $\alpha_{as}$  = apparent physical dispersivity due only to stratification  $k(z)$  (areal conformance=100%), ft or m [L]  
 $\phi$  = porosity, fraction  
 $\Psi = \ln(k/k_{min})$   
 $\tau$  = tortuosity, dimensionless  
 $\sigma$  = standard deviation in probability distribution

## References

- Ayra, A., Hewett, T.A., Larson, R.G. and L.W. Lake, "Dispersion and Reservoir Heterogeneity", SPERE, Feb., 1988.
- Mahadevan, J., Lake, L.W., and R.T. Johns, "Estimation of True Dispersivity in Field Scale Permeable Media", SPE 75247 presented at the SPE/DOE Improved Oil Recovery Symposium, Tulsa, OK, April 13-17, 2002.
- Perkins, T.K., and Johnston, O.C., "A Review of Diffusion and Dispersion in Porous Media", SPEJ (March 1963) 70-84.
- Todd, M.R. and C.A. Chase, "A Numerical Simulator For Predicting Chemical Flood Performance", SPE 7689 presented at the 1979 SPE Symposium on Reservoir Simulation, Denver, CO, Feb. 1-2, 1979.
- Solano, R., Johns, R.T., and L.W. Lake, "Impact of Reservoir Mixing on Recovery in Enriched-Gas Drives Above the Minimum Miscibility Enrichment", SPERE, October, 2001, 358-365
- Stalkup, F., "Predicting the Effect of Continued Gas Enrichment Above the MME on Oil Recovery in Enriched Hydrocarbon Gas Floods", paper SPE 48949 presented at the 1998 SPE Annual Technical Conference and Exhibition, New Orleans, Sept. 27-30.
- Johns, R.T., Pashupati, S., and S.K. Subramanian, "Effect of Gas Enrichment Above the MME on Oil Recovery in Enriched-Gas Floods", SPEJ, Sept. 2000, 331-338.
- Shrivastava, V.K., Nghiem, L.X., and R.G. Moore, "A Novel Approach for Incorporating Physical Dispersion in Miscible Displacement", SPE77724 presented at the SPE Annual Technical Conference and Exhibition, San Antonio, TX, Sept. 29 – Oct. 2, 2002
- Mercado, A., "The Spreading Pattern of Injected Water in a Permeability Stratified Aquifer", Ins. Assoc. Sci. Hydrol. Publ., 72,23-36,1967.
- Kossack, C.A., "The Dispersive Effect of Variable Layer Lengths on Miscible Displacements in Layered Heterogeneous Porous Media", SPERE, May, 1989, 165-170.
- Warren, J.E., and F.W. Skiba, "Macroscopic Dispersion", SPEJ, Sept. 1964, 215-230.
- Pickens, J.F. and G.E. Grisak, "Scale-Dependent Dispersion in a Stratified Granular Aquifer", Water Resources Research, Vol. 4, pp 1191-1211, August 1981.
- Aronofsky, J.W. and Heller, J.P., "Diffusion Model to Explain Mixing of Flowing Miscible Fluids in Porous Media", Trans. AIME (1957) Vol 210, 345.
- Muskat, Morris, "Effect of Permeability Stratification in Cycling Operations", Trans. AIME (1949) 179 313-328.
- Morel-Seytoux, H.J., "Analytical Numerical Method in Waterflooding Predictions", SPEJ Sept. 1965, 247.
- Hagoort, Jacques, "The Response of Interwell Tracer Tests in Watered-Out Reservoirs", SPE 11131 presented at the 57th Annual Fall Technical Conference and Exhibition of the Society of Petroleum Engineers, New Orleans, LA, Sept. 26-29, 1982.
- Gelhar, L.W. and Collins, M.A.: "General Analysis of Longitudinal Dispersion in Nonuniform Flow," Water Resources Res., 7(6), 1511-1521, 1971.
- Tomich, J.F., Dalton, R.L., Jr., Deans, H.A., and L.K. Shallenberger, "Single-Well Tracer Method to Measure Residual Oil Saturation", Trans. AIME (1973) 255, 1211.
- Wellington, S.L., Simone, J.F., Hara, S.K., and E.A. Richardson, "A Single Well Test Method That Yields a Dispersion-Free Measure of Reservoir Fluid Drift Rate", SPE 27757 presented at the DPE/DOE Ninth Symposium on Improved Oil Recovery, Tulsa, OK, April 17-20, 1994
- Coats Engineering Inc., [www.coatsengineering.com](http://www.coatsengineering.com), June, 2004
- Technical Documentation for UTCHEM-7.0—A Three-Dimensional Chemical Flood Simulator, vol. 2, Reservoir Engineering Research Program, Center for Petroleum and Geosystems Engineering, U. of Texas at Austin, Austin, Texas (November 1998).
- StreamSim Technologies, [www.streamsim.com](http://www.streamsim.com), June, 2004
- Greenkorn, R.A., Johnson, C.R. and R.E. Haring, "Miscible Displacement in a Controlled Natural System", Trans. AIME (1965) 234 1329.
- J. Mahavedan, Personal Communication, Jan., 2004
- Pickens, J.F., Merritt, W.F., and Cherry, J.A.: "Field Determination of the Physical Contaminant Transport Parameters in a Sandy Aquifer," *Nuclear Techniques in Water Pollution Studies, Proceedings of Advisory Group Meeting*, Dec. 6-9, 1976, Cracow, Poland, 239-265, International Atomic Energy Agency, Vienna, 1980.

## Appendix. Additive Dispersivities

We have made the following observations based on simulations using the Muskat Eq. 12, then fitting the generated  $C(Q_D)$  results to the CD Eq. 3. First, the total apparent dispersivity  $\alpha_a$  is approximately the sum of physical dispersivity and apparent dispersivity due to conformance,

$$\alpha_a \approx \alpha + \alpha_{ac} \dots\dots\dots (A-1)$$

Second, we found that

$$\alpha_{ac} \approx \alpha_{ap} + \alpha_{as} \dots\dots\dots (A-2)$$

where  $\alpha_{ap}$  is the apparent dispersivity due *only* to areal pattern conformance, and  $\alpha_{as}$  is the apparent dispersivity due *only* to stratification (vertical) conformance.

For all practical purposes,  $\alpha_{ac} \gg \alpha$ , leading to the important observation that

$$\alpha_a \approx \alpha_{ac} \dots\dots\dots (A-3)$$

with the necessary consequence that  $\alpha_a \approx \alpha_{ap} + \alpha_{as}$ .

**Laboratory Apparent Dispersivities.** Lab dispersivity values are obtained from coreflood effluent profiles, using Eq. 3 or another best-fit procedure to obtain apparent dispersivity  $\alpha_a$ . If

the core were homogeneous then  $\alpha_a$  would equal the physical dispersivity  $\alpha$ . Since any core will have some heterogeneity, the effluent profile and its associated  $\alpha_a$  will reflect the combined effects of physical dispersivity and heterogeneity. Let  $\alpha_{ac}$  denote the dispersivity resulting from conformance (heterogeneity) alone (no dispersion,  $\alpha=0$ ) and  $\alpha$  the physical dispersivity (no heterogeneity). Are the dispersivities additive?

We try to answer this question using a stratified model and the Muskat solution with  $F$  given by the CD Eq. 3. Let  $k(z)$  be described by Eq. 11 with  $V=0.13$  and assume physical dispersivity  $\alpha=0.01$  ft. The purely dispersive profile of Eq. 3 for  $\alpha=0.01$  ft is given by a Peclet number  $N_{Pe}=L/\alpha=100$  (using  $L=1$  ft). Using the Muskat solution Eq. 12 for  $V=0.13$ , where  $F(Q_D)$  is a step function  $C=0$  for  $Q_D<1$  and  $C=1$  for  $Q_D\geq 1$ , corresponding to  $\alpha=0$ , gives a Peclet number  $N_{Peac}=103$  from Eq. 3. Using the Muskat solution with  $V=0.13$  and  $F(Q_D)=C$  from Eq. 3 with  $\alpha=0.01$  gives the solution reflecting the combined, simultaneously-acting effects of heterogeneity and dispersion; the apparent Peclet number  $N_{Pe}$  is 50.6. Eq. A-1 is equivalent to

$$N_{Pea}^{-1} = N_{Peac}^{-1} + N_{Pe}^{-1} \dots\dots\dots (A-5)$$

because  $N_{Pe}^{-1}$  is  $\alpha/L$  and  $L$  cancels out. The above Peclet numbers give

$$N_{Pea}^{-1} = 0.01977 = N_{Peac}^{-1} + N_{Pe}^{-1} = 0.00974 + 0.01 = 0.01974$$

affirming Eq. A-1. The same analysis is used for a more heterogeneous  $V=0.4$ . The three respective Peclet numbers,  $N_{Pe}=100$ ,  $N_{Peac}=7.397$ , and  $N_{Pea}=6.839$ , used in Eq. A-1 yield

$$N_{Pea}^{-1} = 0.1462 = N_{Peac}^{-1} + N_{Pe}^{-1} = 0.1352 + 0.01 = 0.1452$$

again affirming Eq. A-1. The coreflood profile Peclet number  $N_{Pea}=6.839$  gives an apparent dispersivity (if  $L=1$  ft)  $\alpha_a=0.1462$  ft, about 15 times larger than the physical dispersivity.

The fact that many reported corefloods yield near-S-shape profiles with dispersivities  $\sim 0.01$  ft arguably implies those cores are homogeneous or nearly so, with  $\alpha_{ac}/\alpha < \text{or} \ll 1$ .

One might argue that the effects of heterogeneity on lab-measured dispersivity make its value uncertain, even to the point of disputing its acceptance as a rock property independent of scale and time. The same argument could be used to dispute permeability as a rock property, since coreplug heterogeneity will affect measured permeability just as it affects measured dispersivity.

**Additive Conformance Dispersivities.** Using the same approach described in the previous section for showing how physical and stratification dispersivities are additive, a similar exercise was made to test if areal pattern and stratification dispersivities are also additive.

Consider again the results shown in Fig. 7, as discussed in the section *Stratified Five-Spot*. The open black circles connected with a thin black line represent apparent Peclet numbers estimated using additive conformance dispersivities, Eq. A-2, for a wide range of stratification from  $V=0$  to 0.9. The stratified five-spot  $C(Q_D)$  from the Muskat solution gives

the combined, simultaneously-acting effects of areal pattern conformance and stratification (vertical) conformance. Fitting this solution to the 1D CD Eq. 3 yields the apparent Peclet numbers shown as a solid black line in Fig. 7. The maximum error in estimated apparent Peclet number using additive dispersivities is 7%, being exact for  $V=0$ .

L m	SW1 Rate			Half SW1 Rate		
	$t_{inj}$ days	$\alpha_a$ m	$N_{Pea}$	$t_{inj}$ days	$\alpha_a$ m	$N_{Pea}$
5.6	1	0.018	315.6	2	0.052	106.9
9.7	3	0.061	158.6	6	0.228	42.6
11.9	4.5	0.108	109.9	9	0.452	26.3
13.7	6	0.163	84.2	12	0.570	24.0
15.8	8	0.245	64.6	16	0.809	19.5

Layer	h (ft)	k (D)
1	1.8	6.75
2	3.2	9.16
3	1.7	8.23

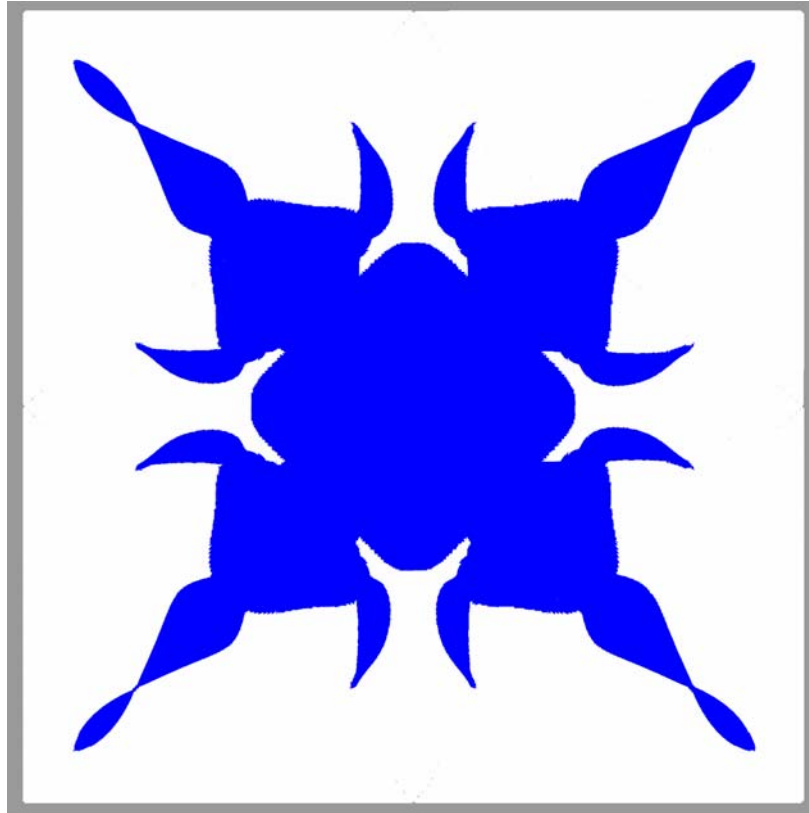


Fig. 1 – Concentration profile (blue=1, white=0) from 3DSL streamline simulation at  $Q_D=0.3366$ , single-layer, 7x7 checkerboard 5-spot pattern with 100:1 permeability ratio and 2:1 porosity ratio in alternating 7x7 square regions (high- $k$  and high- $\phi$  squares at corners).

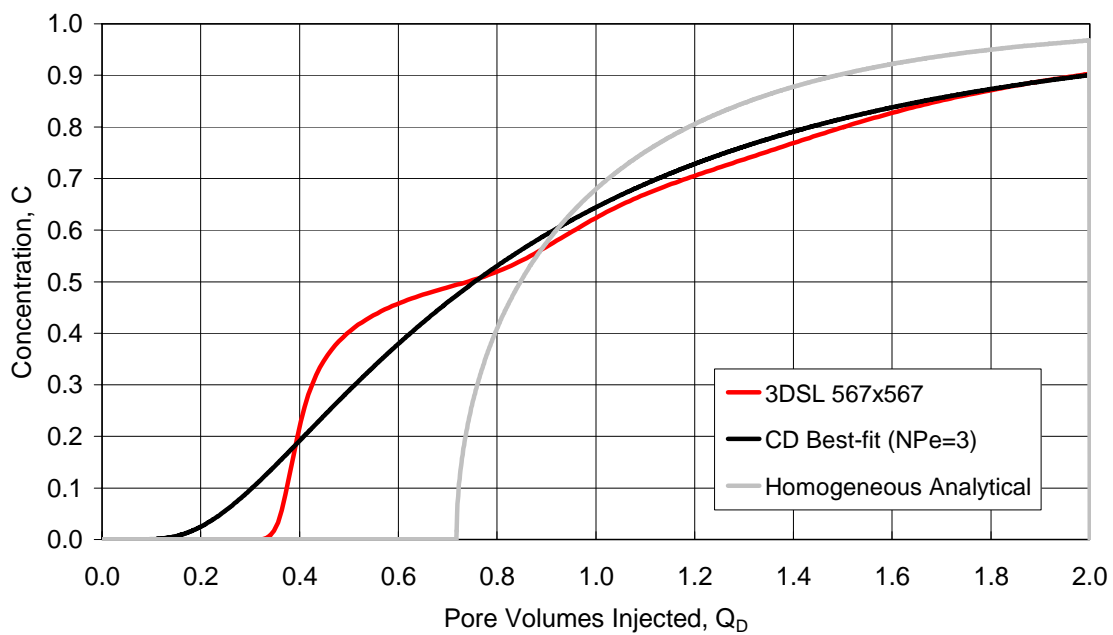


Fig. 2 – Single-layer checkerboard 5-spot using streamline numerical simulator 3DSL (red line). Best-fit to the CD Eq. 3 with apparent Peclet numbers  $N_{Pea}=3$  (black line). Comparison with single-layer homogeneous 5-spot (gray line).

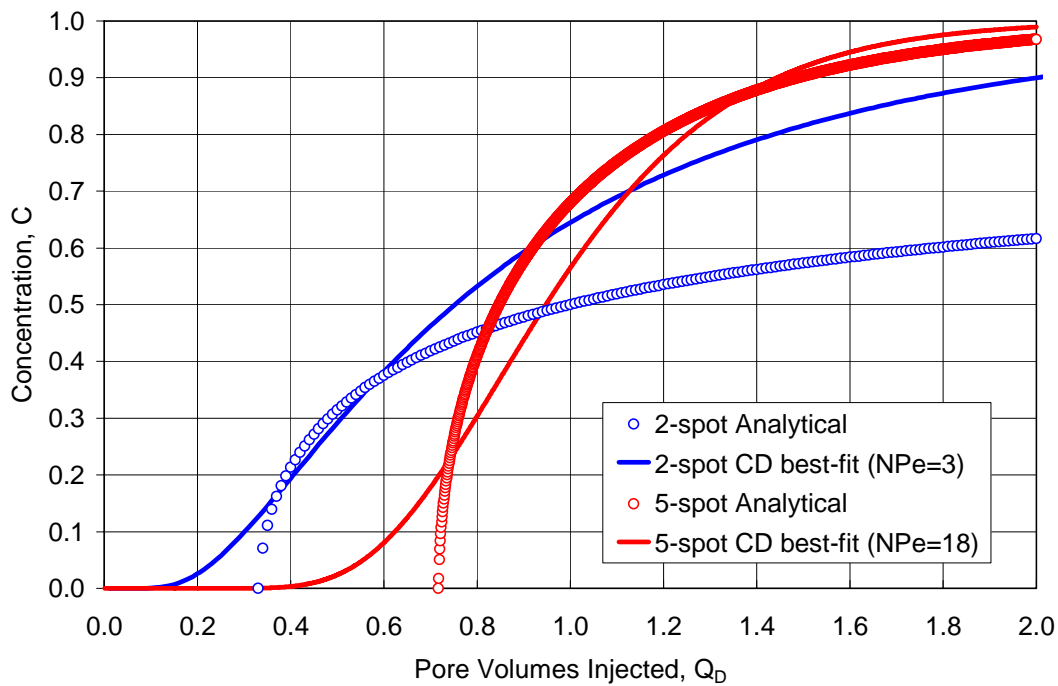


Fig. 3 – Single-layer 2-spot and 5-spot  $C(Q_D)$  profiles from analytical solutions. Best-fit to the CD Eq. 3 with apparent Peclet numbers  $N_{Pea}=3$  and 18, respectively. Zero physical dispersion.

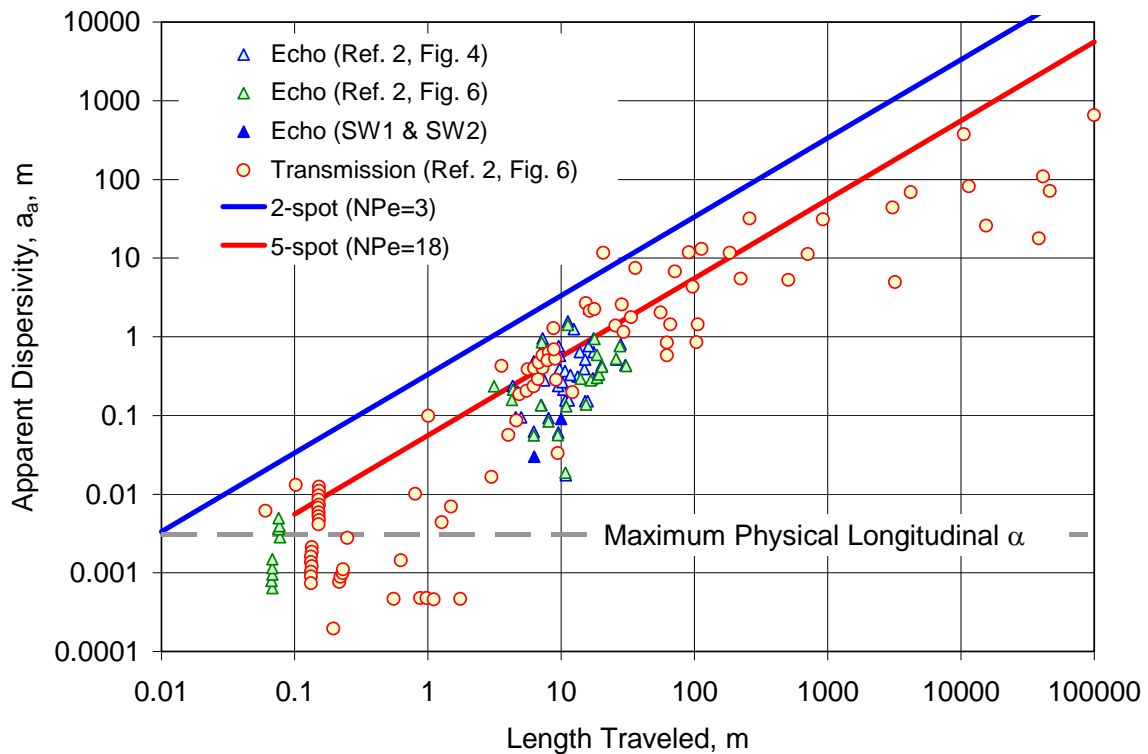


Fig. 4 – Apparent dispersivity scale dependence with length traveled. Reported literature best-fit CD data (symbols) and expected linear trend for constant  $N_{Pe}$  values in 1D CD Eq. 3, representing areal conformance (only) for 2-spot and 5-spot.

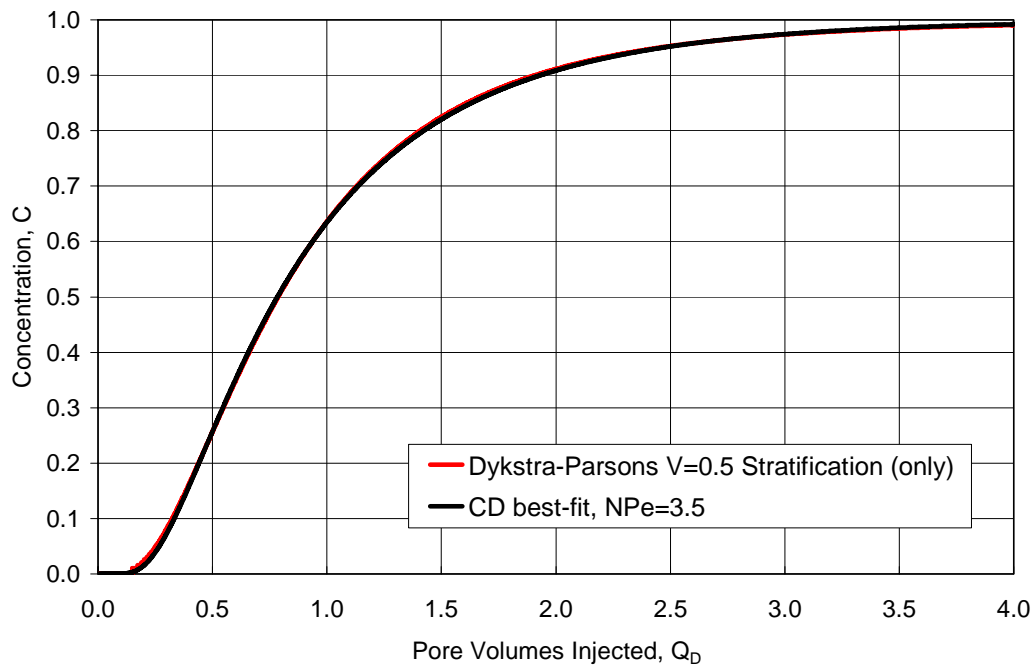


Fig. 5 – Best-fit CD match of  $N_{Pe}=3.5$  to log-normal Dykstra-Parsons  $V=0.5$  stratification (red line); 100% areal conformance assumed.

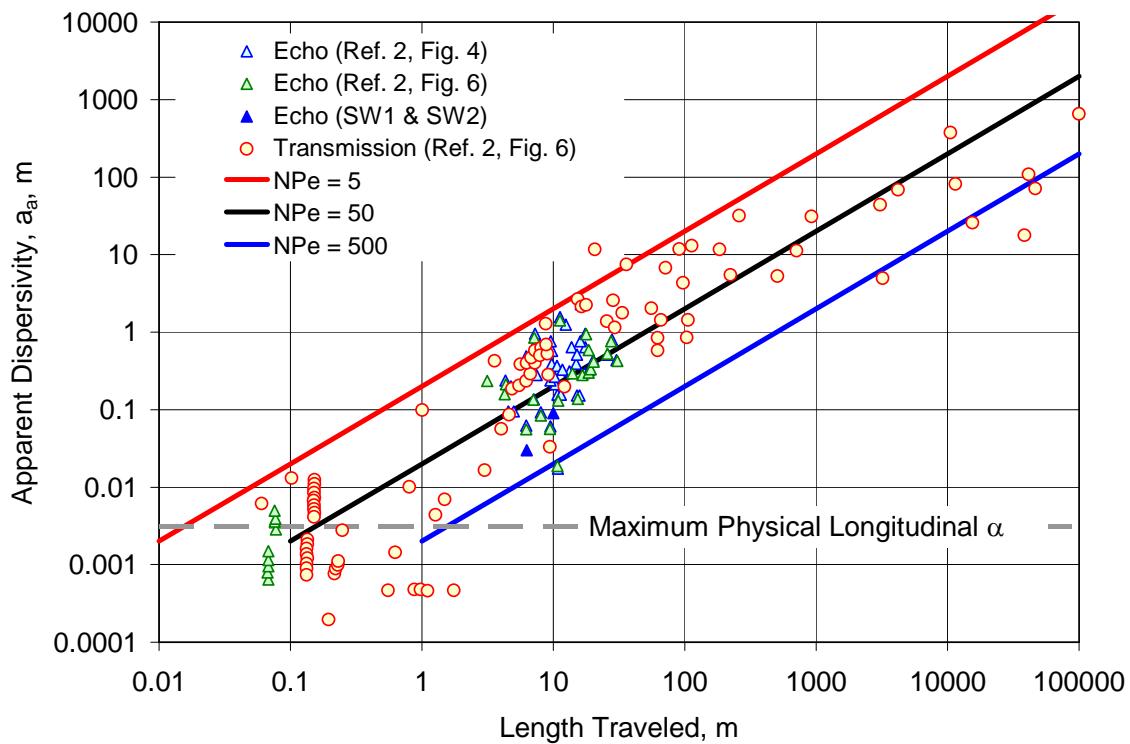


Fig. 6 – Apparent dispersivity scale dependence with length traveled. Reported literature best-fit CD data (symbols) and expected linear trend for constant  $N_{Pe}$  values in 1D CD Eq. 3.

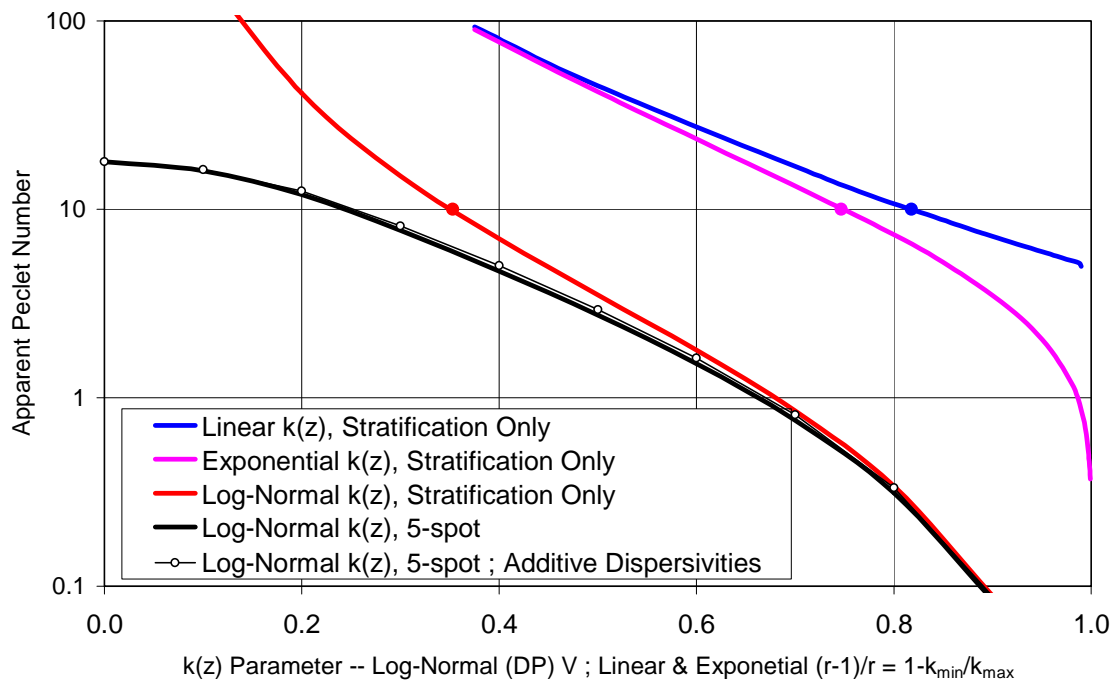


Fig. 7 – Apparent Peclet number relation to stratification parameters (100% areal conformance assumed): log-normal Dykstra-Parsons  $V$  (red line); Muskat linear and exponential models  $(r-1)/r=1-k_{min}/k_{max}$  (blue and pink lines). Also shown is the composite 5-spot areal with log-normal stratification (black line) conformance, with additive dispersivity approximation (black circles).

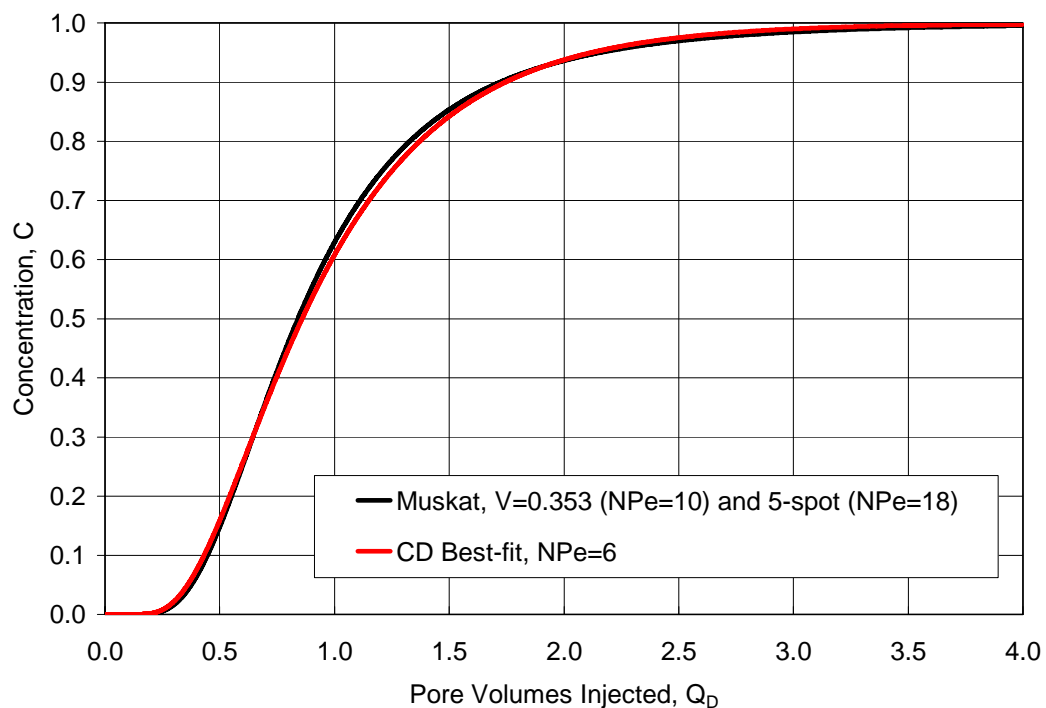


Fig. 8 – Muskat solution to 5-spot ( $N_{pea}=18$ ) with Dykstra-Parsons  $V=0.353$  stratification ( $N_{pea}=10$ ), having CD best-fit  $N_{pea}=6$ .

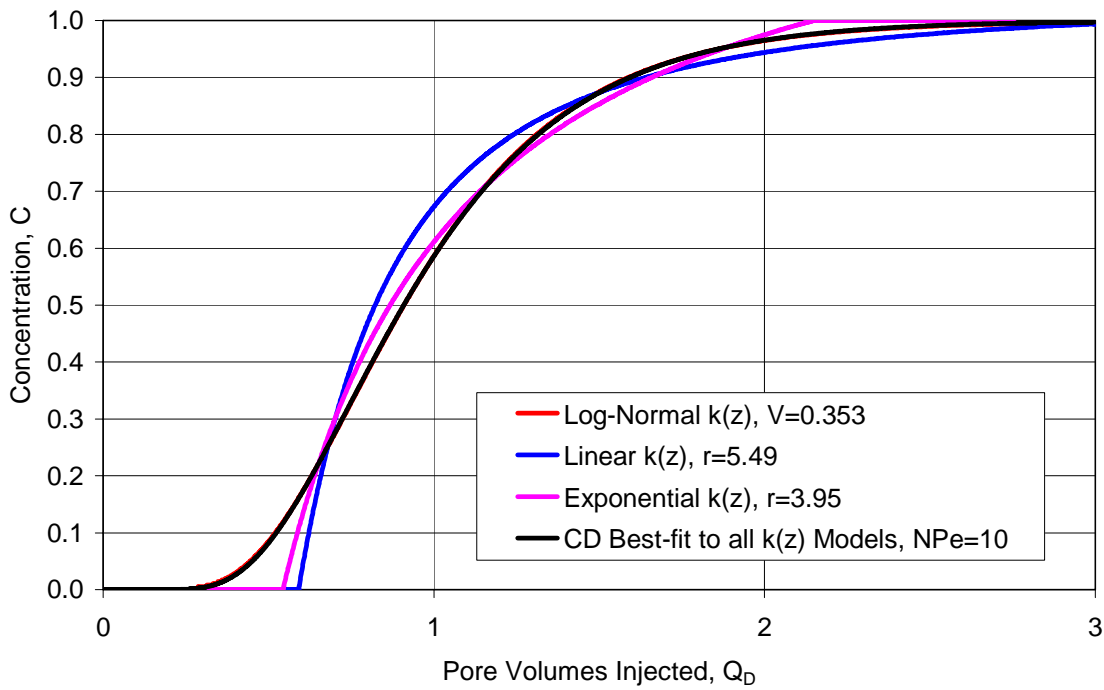


Fig. 9 – Best-fit CD match of  $N_{Pe}=10$  to three stratification  $C(Q_D)$  relations (100% conformance assumed): log-normal Dykstra-Parsons  $V$  (red line); Muskat linear and exponential models (blue and pink lines). Best-fit CD and  $V=0.353$  log-normal curves are coincident (near-perfect fit).

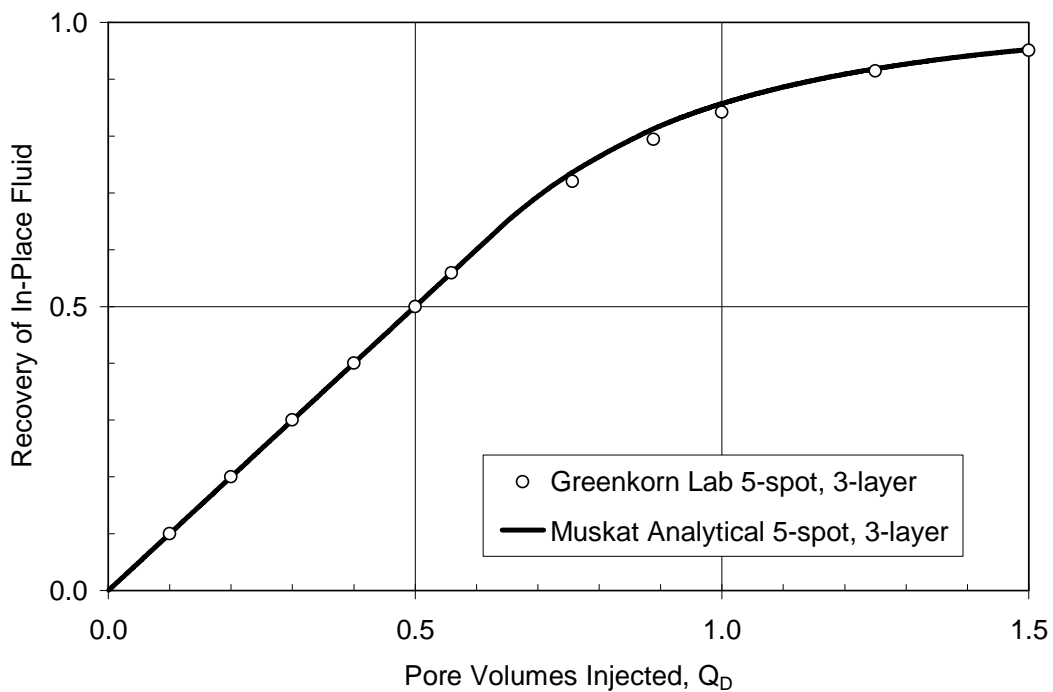


Fig. 10 – Prediction of recovery performance of a laboratory 5-spot, 3-layer tracer test<sup>23</sup> using the Muskat Eq. 12 analytical solution for a 5-spot pattern and lab layer properties.

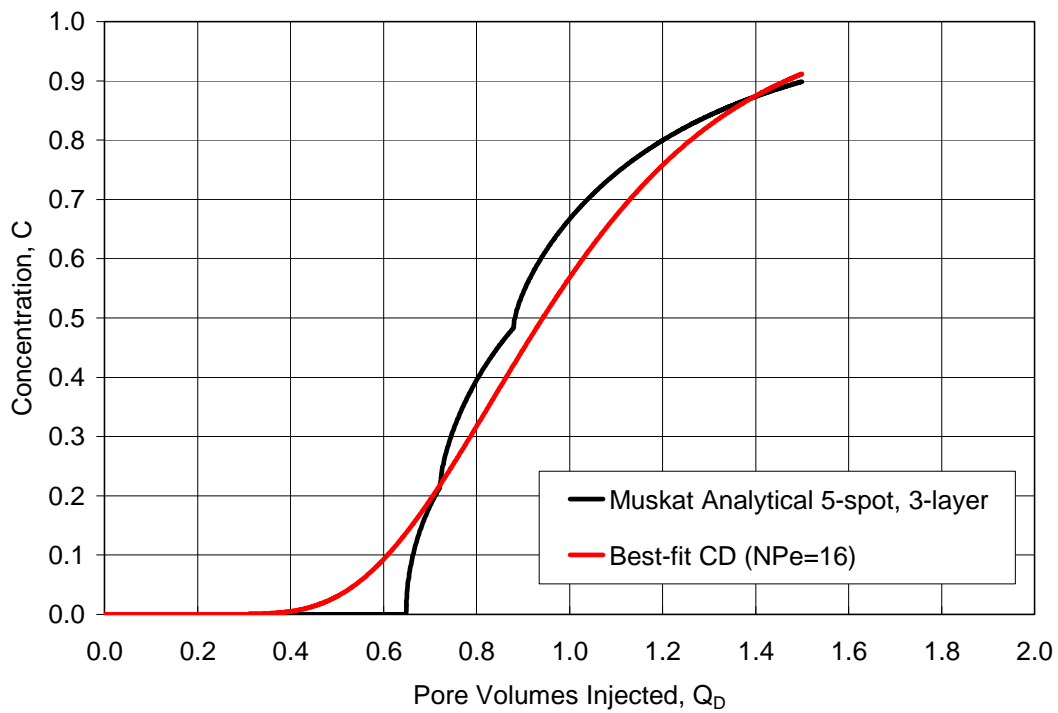


Fig. 11 – CD best-fit of the Muskat Eq. 12 analytical solution for a 5-spot pattern and lab layer properties describing the Greenkorn<sup>23</sup> laboratory test.

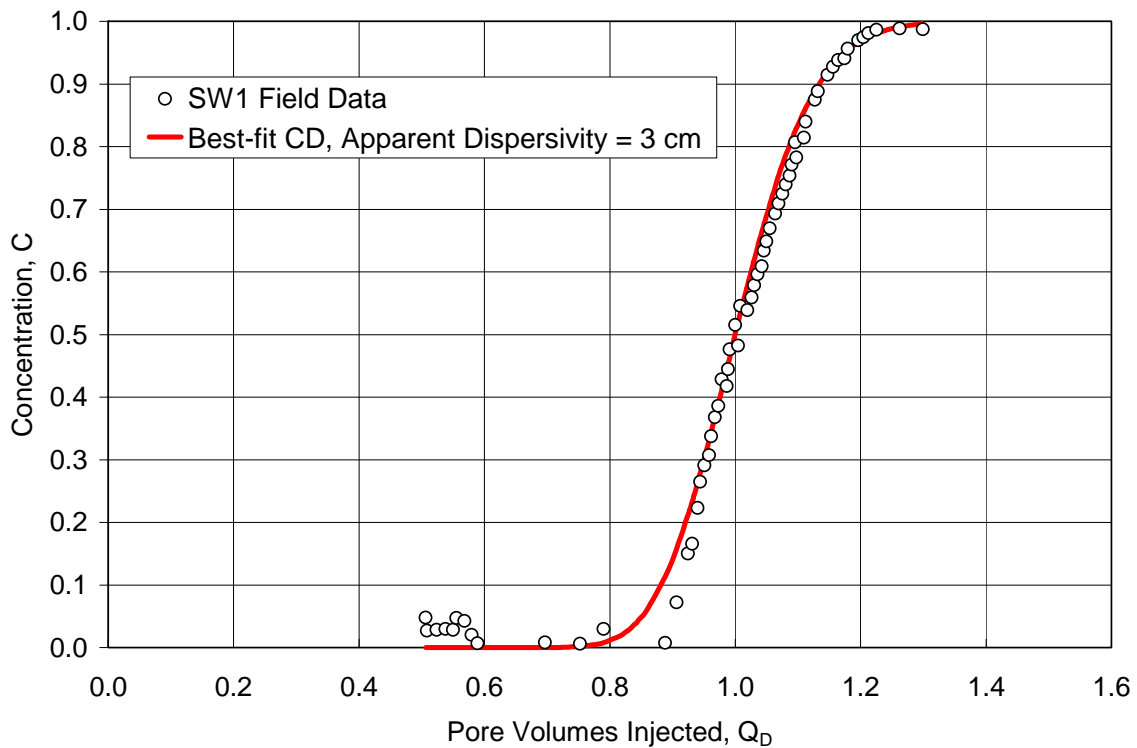


Fig. 12 – Pickens-Grisak SW1 test data and best-fit CD model with  $N_{Pea}=209$ ,  $\alpha_a=3$  cm.

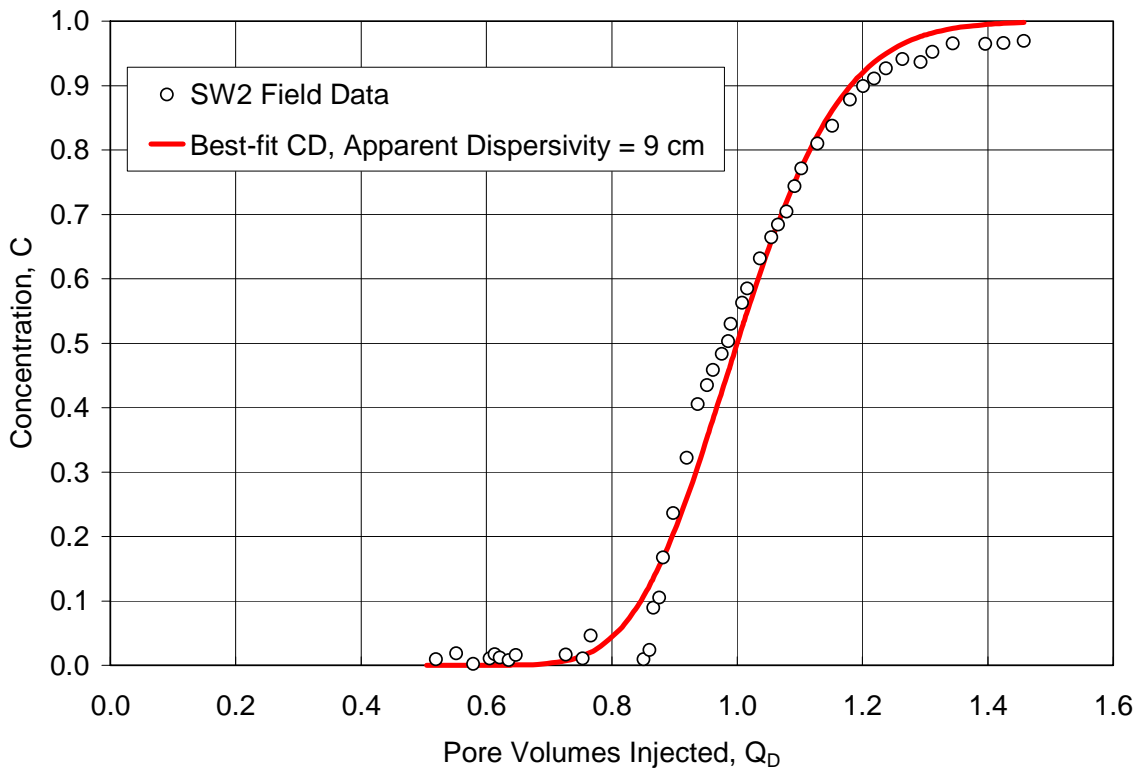


Fig. 13 – Pickens-Grisak SW2 test data and best-fit CD model with  $N_{pea}=118$ ,  $\alpha_a=9$  cm.

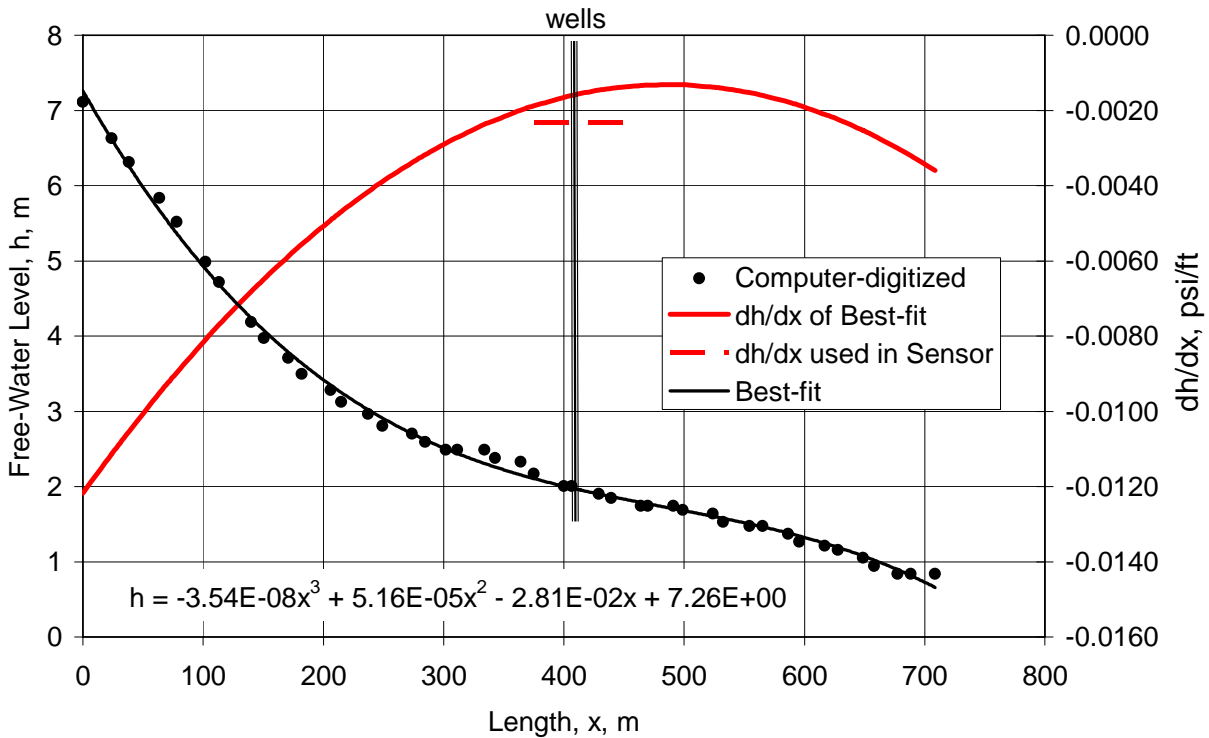


Fig. 14 – Pickens-Grisak well test data for estimating drift gradient used in SW1, SW2, and two-well modeling.

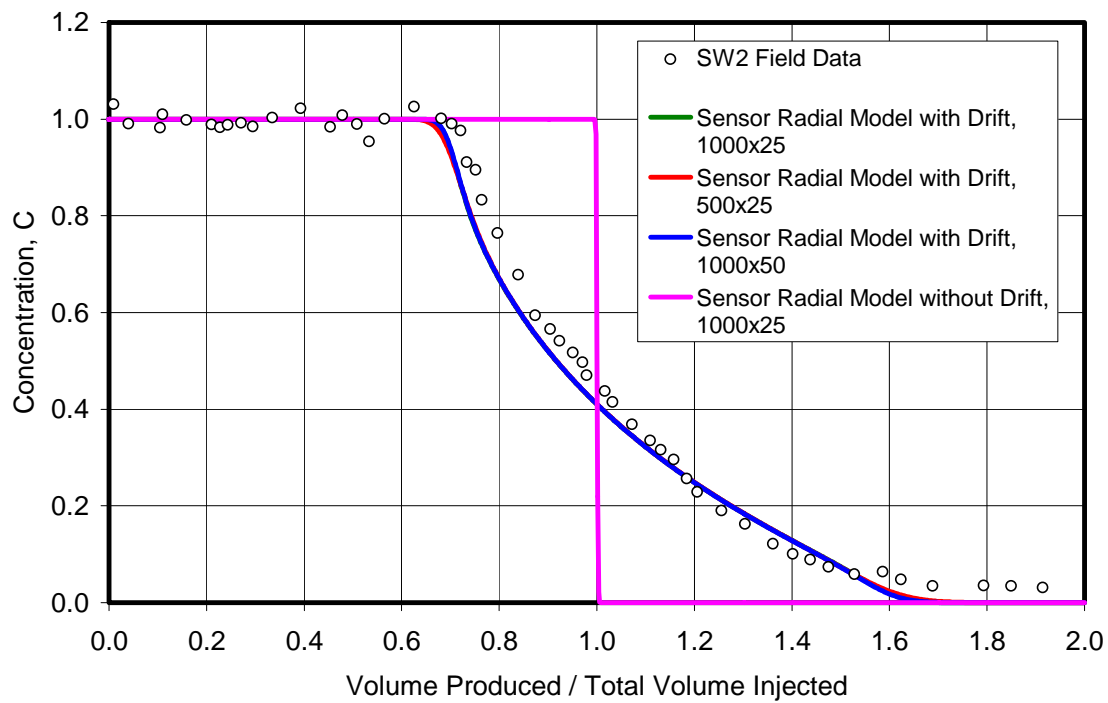


Fig. 15 – Pickens-Grisak SW2 test data and Sensor  $r$ - $\theta$ - $z$  model with drift, with zero numerical dispersion (CFL=1).

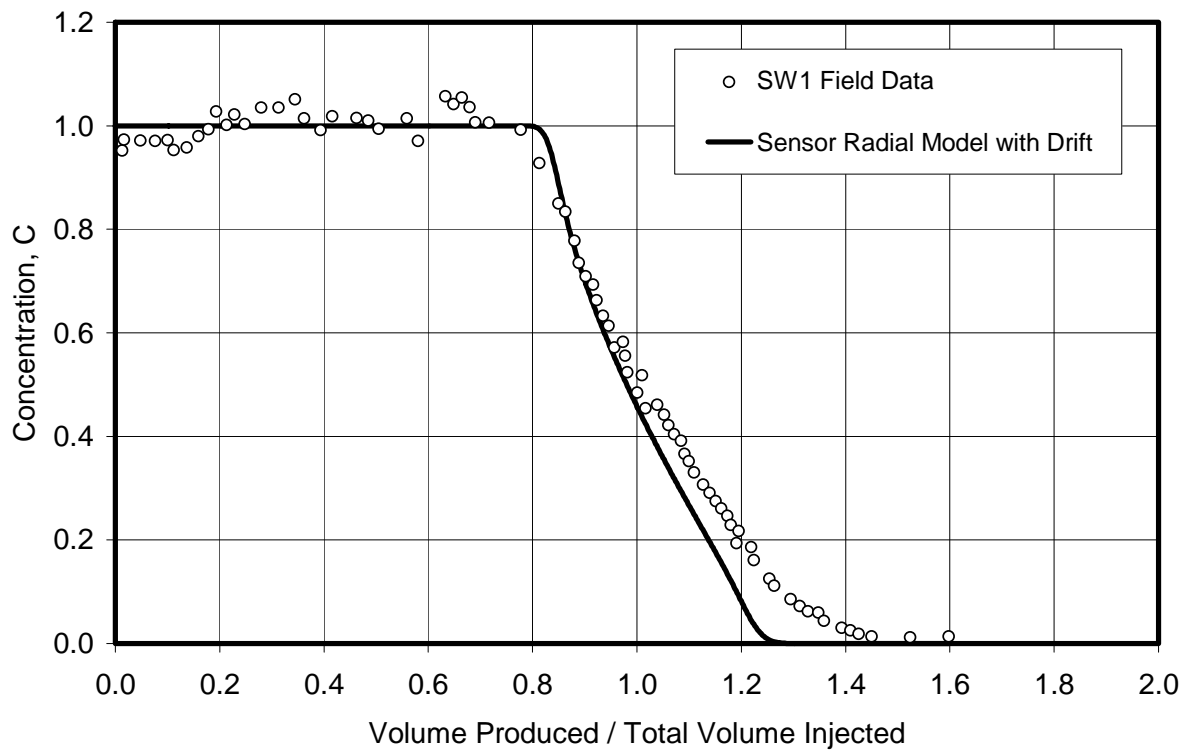


Fig. 16 – Pickens-Grisak SW1 test data and Sensor  $r$ - $\theta$ - $z$  model with drift.

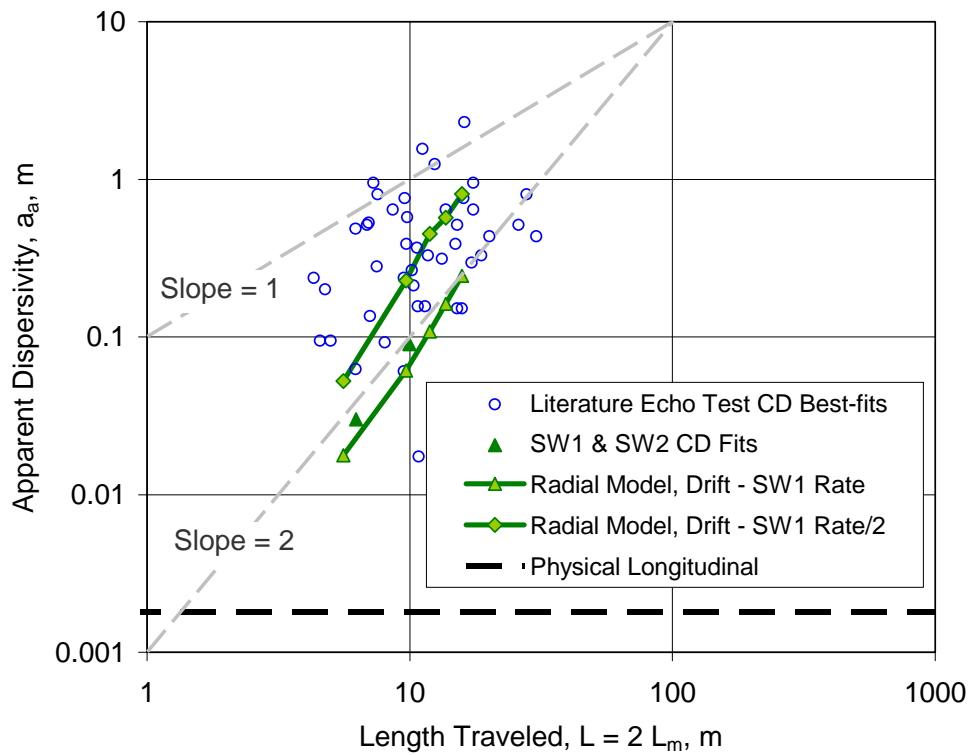


Fig. 17 – Apparent dispersivity scale dependence for echo tests. Literature data (symbols) and Sensor simulated trends for Pickens-Grisak SW area wells with drift using two injection=production rates with varying injection periods.

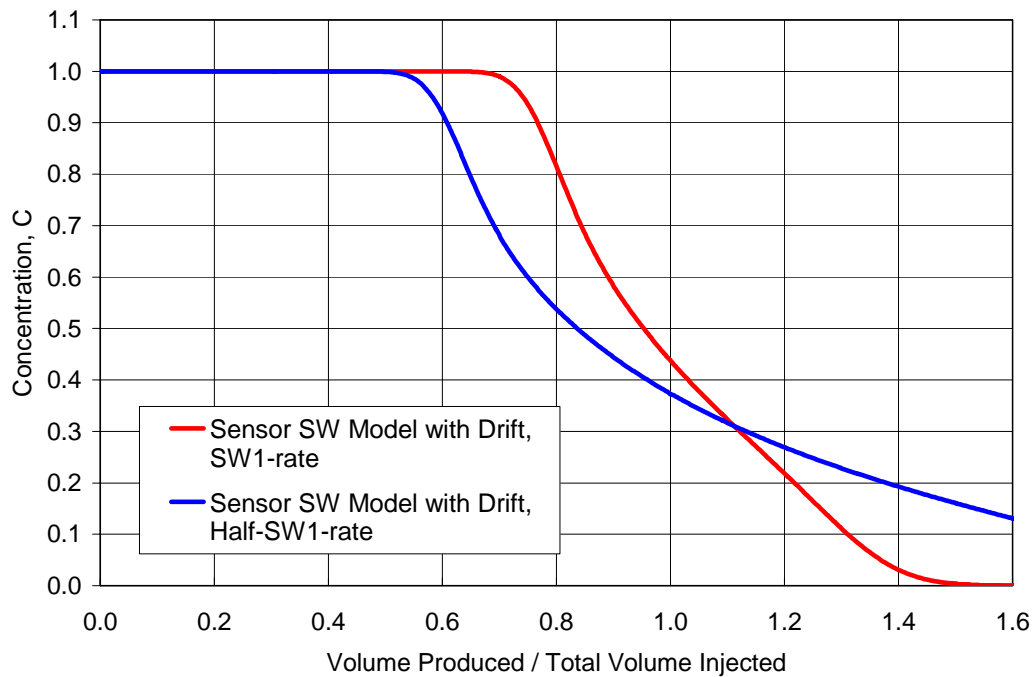


Fig. 18 – Pickens-Grisak SW test area, Sensor model predictions with drift for two injection=production rates;  $L_m=9.7$  m (3 days at SW1-rate, 6 days at half-SW1-rate).

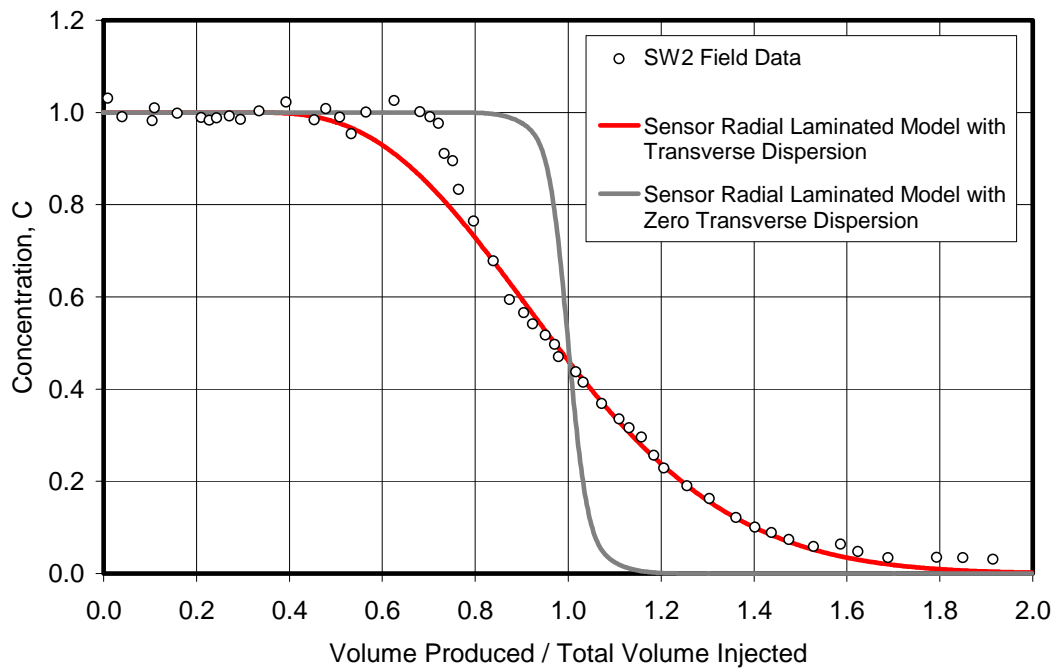


Fig. 19 – Pickens-Grisak SW2 test data and Sensor  $r$ - $\theta$ - $z$  model with thin laminations (2.44 cm) having 3:1  $k$ -contrast,  $\alpha_t=0.0035$  cm,  $D_0=2 \cdot 10^{-5}$  cm<sup>2</sup>/s; no drift, and only minor (<2%) numerical dispersion.

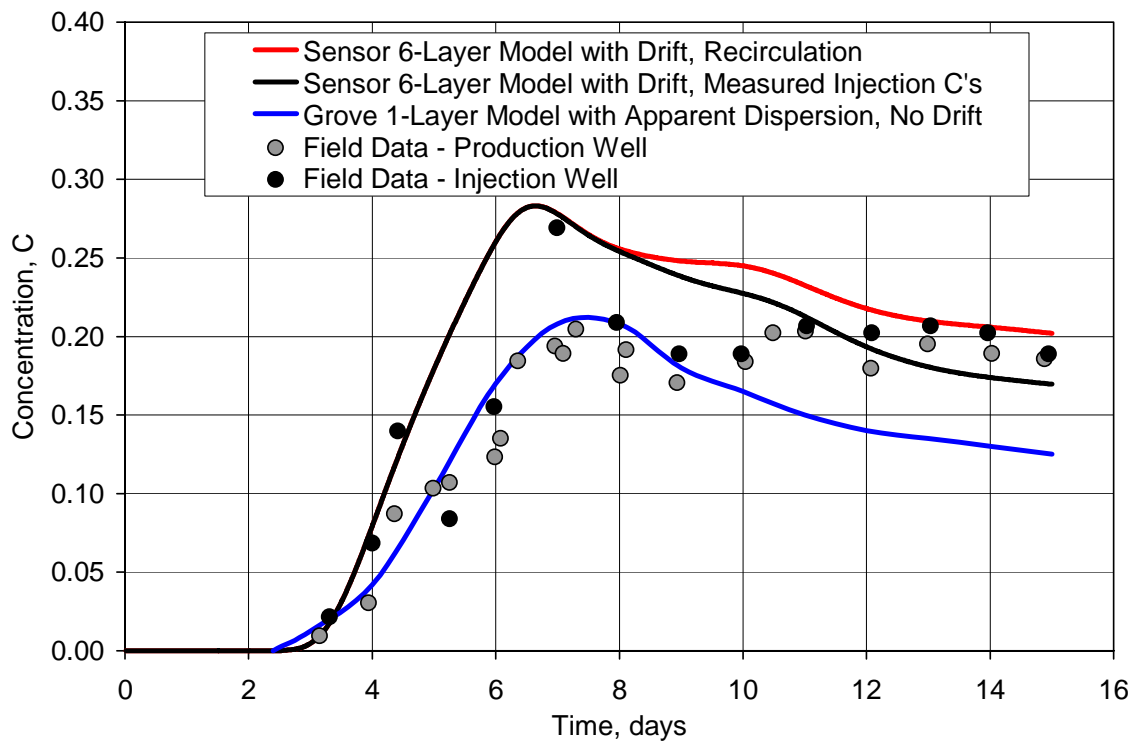


Fig. 20 – Pickens-Grisak two-well transmission test results, with recycling of produced tracer. Comparison of Sensor  $r$ - $\theta$ - $z$  model with measured stratification and drift for (a) re-injection of model-produced water (red line) and (b) injecting field-measured concentrations (black line); also, single-layer 2-spot solution without drift and using apparent dispersivity (Grove model<sup>12</sup>).

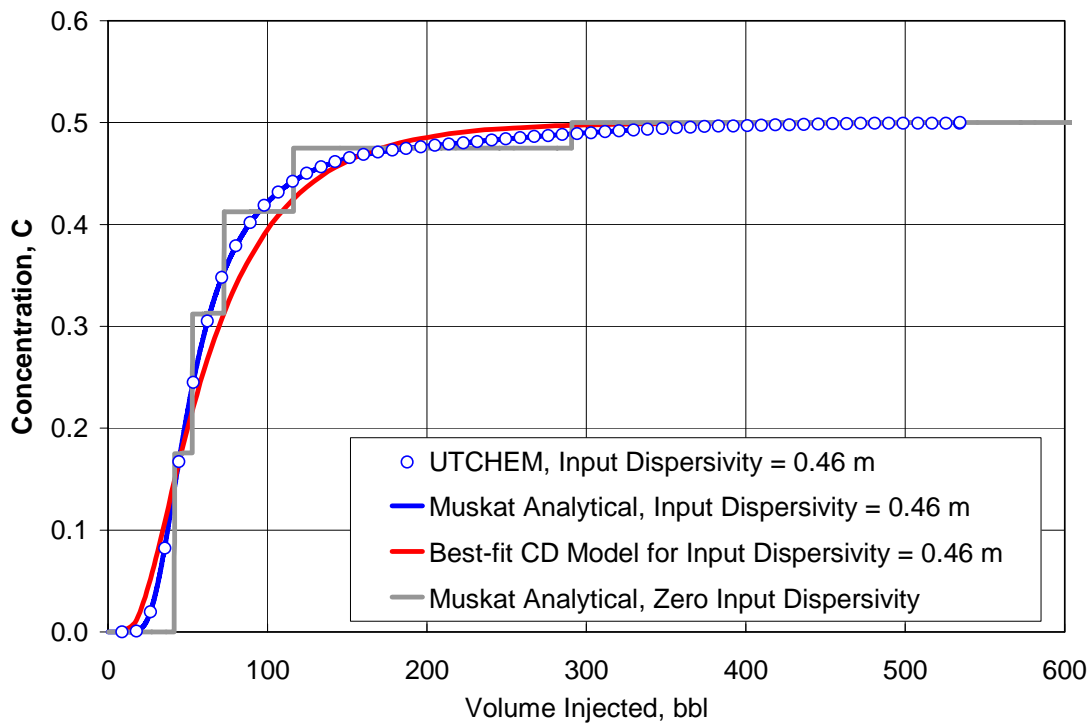


Fig. 21 – Mahadevan et al.<sup>2</sup> 5-layer  $x$ - $z$  cross-section transmission test with input dispersivity 0.46 m, comparing UTCHEM numerical solution (blue circles) with Muskat Eq. 12 analytical model (blue line). Zero-dispersion solution (gray line). Best-fit CD model for input  $\alpha=0.46$  m is  $N_{pe}=2.24$  (red line).

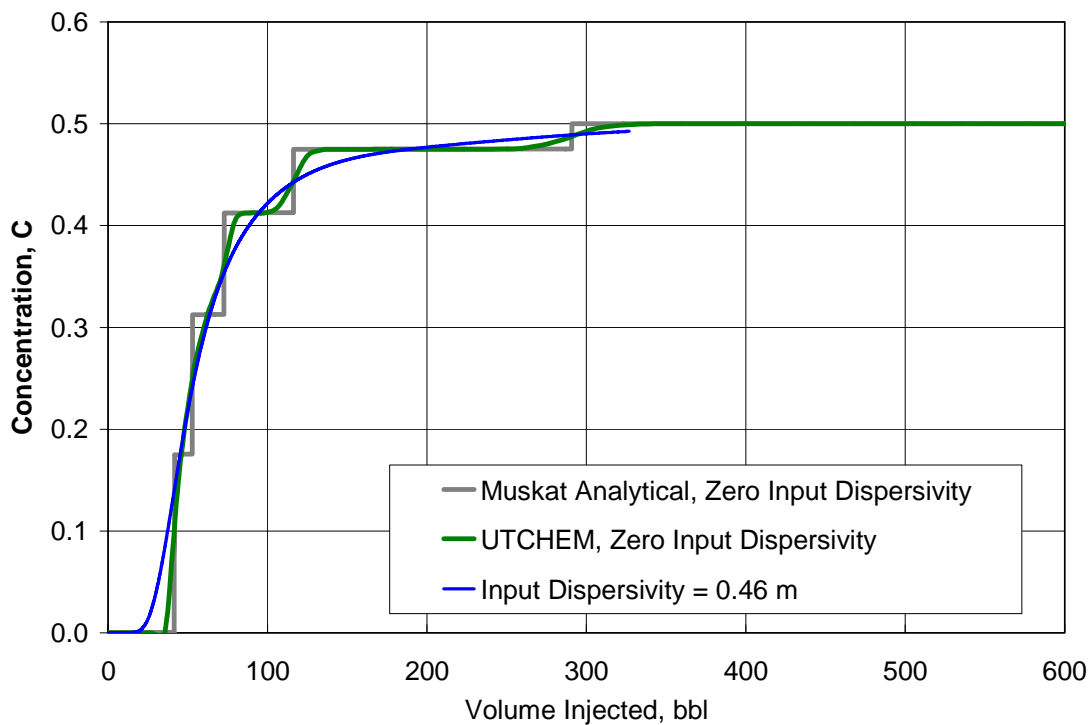


Fig. 22 – Mahadevan et al.<sup>2</sup> 5-layer  $x$ - $z$  cross-section transmission test with zero input dispersivity, comparing analytical Muskat solution (gray line) with UTCHEM TVD higher-order difference scheme (green line); solution with input dispersivity 0.46 m also shown (blue line).

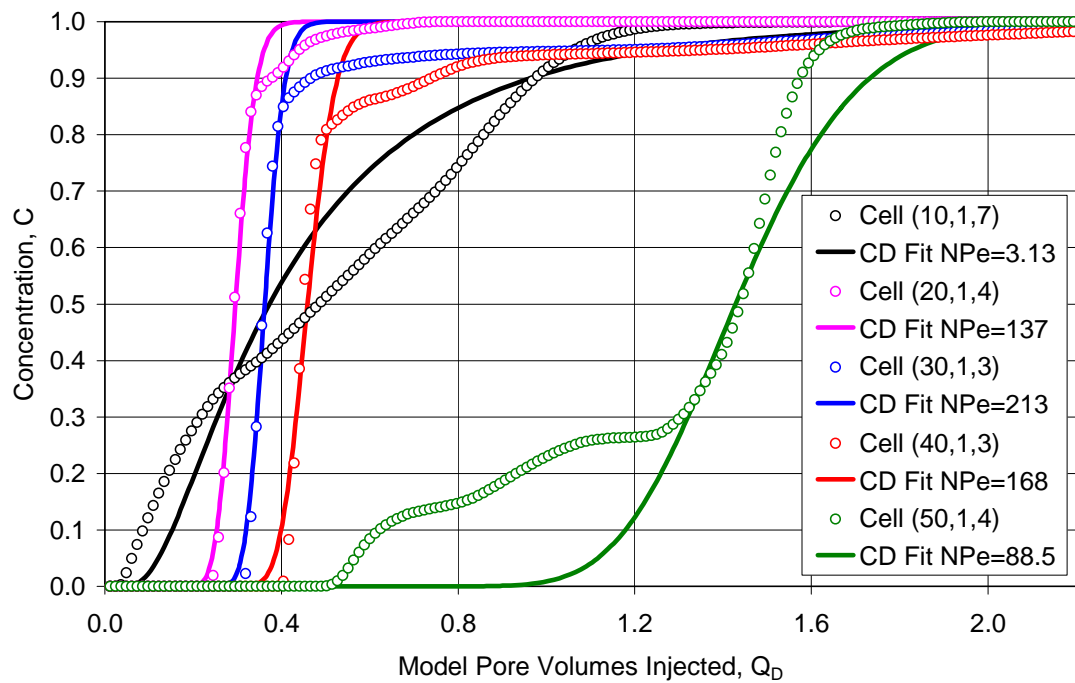


Fig. 23 – Mahadevan et al.<sup>2</sup> UTCHEM 8-layer  $x$ - $z$  cross-section transmission test with zero input dispersivity, showing individual-cell concentration profiles variation during the test. Best-fit CD Eq. 3 lines also shown.

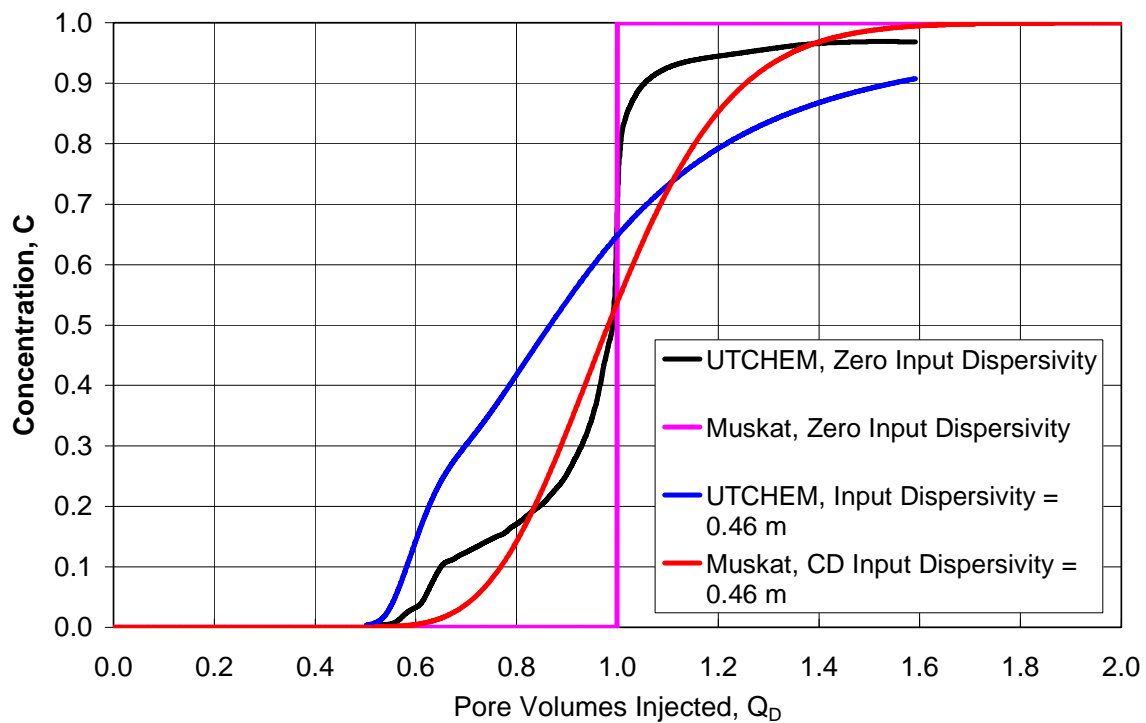


Fig. 24 – Mahadevan et al.<sup>2</sup> UTCHEM 8-layer  $x$ - $z$  cross-section echo test for  $L=80.88$  ft, illustrating numerical dispersion error (black and blue lines). Exact solutions are given by Muskat model (pink and red lines).